Inorganic Chemistry
Cite This: Inorg. Chem. XXXX, XXX, XXX–XXX
Article
pubs.acs.org/IC

Binuclear Double-Stranded Helicates and Their Catalytic Applications in Desymmetrization of Mesodiols

Eswaran Chinnaraja,[†,‡] Rajendran Arunachalam,[†,‡] Eringathodi Suresh,[‡,⊥] Shovan K. Sen,[‡,∥] Ramalingam Natarajan,[‡,∥] and Palani S. Subramanian*[,†,‡]

[†]Inorganic Materials and Catalysis Division and [⊥]Analytical and Environmental Science Division and Centralized Instrument Facility, CSIR-Central Salt and Marine Chemicals Research Institute (CSIR-CSMCRI), Bhavnagar 364 002, Gujarat, India

[‡]Academy of Scientific and Innovative Research (AcSIR), Chennai 600113, Tamil Nadu, India

[∥]Organic & Medicinal Chemistry Division, CSIR-Indian Institute of Chemical Biology, Kolkata 700032, West Bengal, India

Supporting Information

ABSTRACT: The ligand L_1 of 4-methyl-2,6-diformylphenol and L_2 of 4-*tert*-butyl-2,6-diformylphenol are synthesized through Schiff base condensation with *rac*-, (*R*)-(+), or (*S*)-(−)-1,1′-binaphthyl-2,2′-diamine (BNDA). As a result, the racemic L_1^{rac}, L_2^{rac}, and enantiopure L_1^{RR}, L_1^{SS}, L_2^{RR}, and L_2^{SS} ligands are obtained incorporating Cu(II) and Zn(II) salts by a simple one-pot metal template method. The series of dinuclear complexes of $[M_2LX_2]$ (here, M = Cu^{2+}, Zn^{2+}; X = acetate ion, chloride ion; L = L_1^{RR}, L_1^{SS}, L_1^{rac}, L_2^{RR}, L_2^{SS}, L_2^{rac}) formulas are obtained in common. Among them, the single crystal X-ray structures for $[Zn_2L_1^{rac}(OAc)_2]$ and $[Zn_2L_1^{SS}Cl_2]$ complexes are obtained. The detailed crystal structure and the chiroptical studies performed on these complexes dictates a self-sorting behavior in their self-assembly process and illustrate a chirality transfer from the ligand to the metal center on the complexes. The enantiopure dinuclear complexes $[M_2L^{RR}X_2]$ and $[M_2L^{SS}X_2]$ generate enantiopure ΛΛ and ΔΔ isomers, respectively, but the racemic complexes produce only homochiral ΛΛ and ΔΔ assemblies. The detailed studies based on UFLC (Ultra Fast Liquid Chromatography), CD, and single crystal X-ray structure together show the absence of heterochiral ΛΔ mesocate. All these complexes are adapted as catalysts for desymmetrization of various mesodiols, and the enantiopure complexes are found to give efficient enantioselectivity in desymmetrization of mesodiols with benzoyl chloride to monobenzoylated ester providing 98% yield and 92% *ee*.

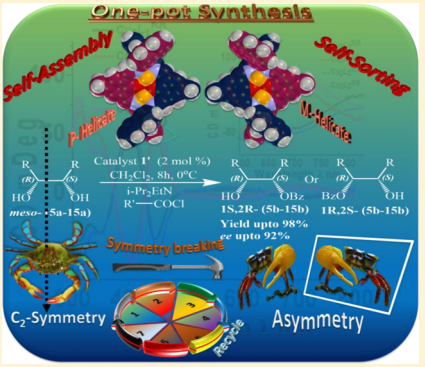

INTRODUCTION

Desymmetrization of secondary diols can be achieved either by kinetic resolution of secondary alcohols (KRSA) or by an enantioselective desymmetrization of mesodiols (EDMD). For enzyme-catalyzed asymmetric acylation,[1,2] although known for its high stereo- and regioselectivity, slow reactivity is its biggest setback. The disadvantages in KRSA are its time consumption, and the yields remain ≤50%. EDMD is found superior to the KRSA, due to its many advantages such as (i) single step, (ii) high yield, and (iii) enantioselectivity up to 100%. EDMD is influenced by two different routes mediated through chiral (i) nucleophilic pathway and (ii) metal catalytic pathway.[3] A number of efficient metal[4] and organocatalysts[5−10] have already been applied to the synthesis of various natural products, building blocks in the asymmetric synthesis of antifungals,[11] sugars,[12] and so forth containing desymmetrized alcohols. Metal complexes of mono- and binuclear Cu(II)[13] and Zn(II)[14] catalysts were also reported for the desymmetrization of mesodiols.[15]

Among the bimetallic complexes, the binuclear helicates possessing attractive double helical architecture, its biochemical relevance to DNA, and the associated chiroptical properties makes them potential candidates.[16] Helicate possessing helical chirality (P/M) when constructed with inbuilt chiral component (*R*/*S*) gains geometrical chirality (Δ/Λ) and deserves additional advantages because of the enhanced chiral components.[17] Although such helicates are rich in the literature, they are rarely explored in the asymmetric catalysis.[18] With this in mind, by adapting *rac*-, (*R*)-(+), or (*S*)-(−)-1,1′-binaphthyl-2,2′-diamine (BNDA) with the appropriate dialdehyde mentioned above, a series of binuclear double-stranded helicates of the type $[M_2LX_2]$ (here M = Cu^{2+}, Zn^{2+}; X = OAc^-, Cl^-; L = L_1^{RR}, L_1^{SS}, L_1^{rac}, L_2^{RR}, L_2^{SS}, L_2^{rac}) incorporating Cu(II) and Zn(II) salts were synthesized as shown in Scheme 1. The detailed chiroptical studies on these complexes explore an interesting self-sorting behavior by selectively forming homochiral ΔΔ and ΛΛ pairs. With monoacylation of symmetric diols being a challenging reaction in organic asymmetric transformations, these enantiopure binuclear double-stranded helicates are intensively investigated in the present work for their catalytic role in selective

Received: December 31, 2018

DOI: 10.1021/acs.inorgchem.8b03643
Inorg. Chem. XXXX, XXX, XXX–XXX

Scheme 1. Synthesis of $[M_2LX_2]$ Type Binuclear Terminally Closed Helicates by Metal Template Method

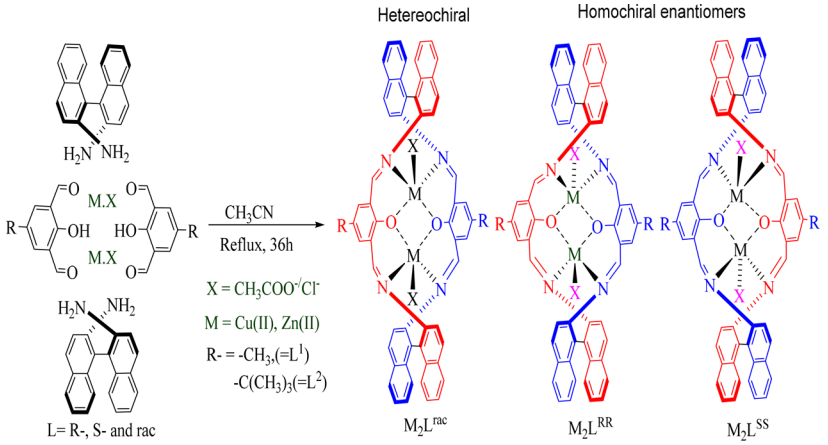

M	-R	$[M_2[L^{rac}.X_2]$	$[M_2L^{RR}.X_2]$	$[M_2[L^{SS}.X_2]$
Cu(II)	$-CH_3$	$[Cu_2L_1^{rac}.X_2]$ (**1**)	$[Cu_2L_1^{RR}.X_2]$ (**1′**)	$[Cu_2L_1^{SS}.X_2]$ (**1″**)
Cu(II)	$-C(CH_3)_3$	$[Cu_2L_2^{rac}.X_2]$ (**2**)	$[Cu_2L_2^{RR}.X_2]$ (**2′**)	$[Cu_2L_2^{SS}.X_2]$ (**2″**)
Zn(II)	$-CH_3$	$[Zn_2L_1^{rac}.X_2]$ (**3**)	$[Zn_2L_1^{RR}.X_2]$ (**3′**)	$[Zn_2L_1^{SS}.X_2]$ (**3″**)
Zn(II)	$-C(CH_3)_3$	$[Zn_2L_2^{rac}.X_2]$ (**4**)	$[Zn_2L_2^{RR}.X_2]$ (**4′**)	$[Zn_2L_2^{SS}.X_2]$ (**4″**)

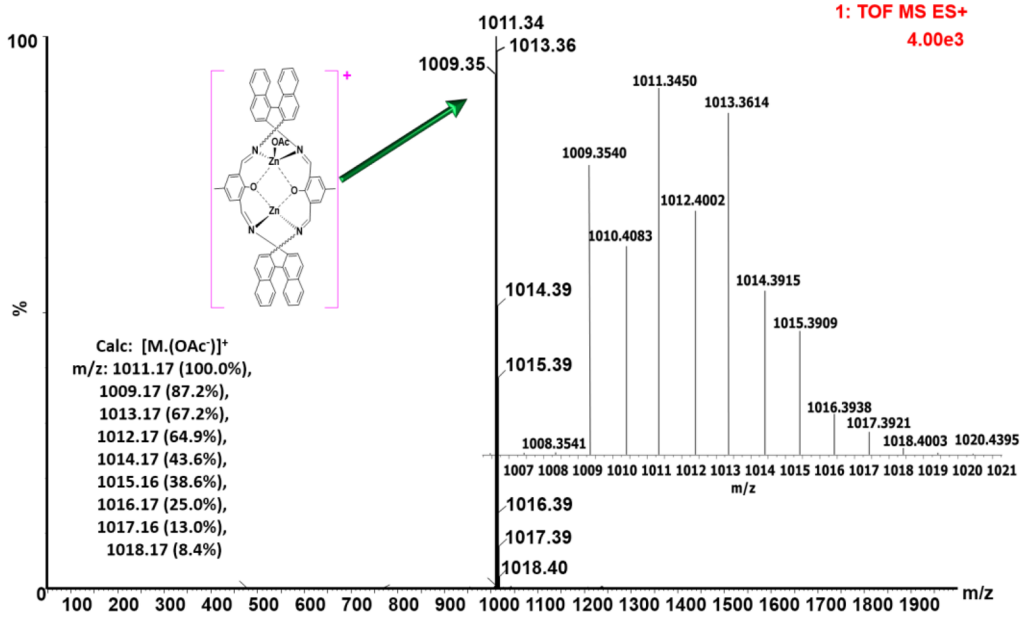

Figure 1. $[ESI\text{-}MS]^+$ spectra of $[Zn_2L_1^{rac}(OAc)_2]$ (**3**) (inset shows the isotopic distribution pattern).

desymmetrization of mesodiols. The structure−reactivity correlation between the helical structure of the complexes and its role in favoring the desymmetrization is also discussed in detail.

RESULTS AND DISCUSSION

The binaphthyl moiety is known for its unique structural rigidity and intrinsic axial chirality. By incorporating *rac*-, (*R*)-(+)-, or (*S*)-(−)-1,1′-BNDA with 4-methyl-2,6-diformylphenol or 4-*tert*-butyl-2,6-diformylphenol and metal salts, a series of binuclear double-stranded helicates $[Cu_2L_1^{rac}\ X_2]$ (**1**), $[Cu_2L_1^{RR}\ X_2]$ (**1′**), $[Cu_2L_1^{SS}\ X_2]$ (**1″**), $[Cu_2L_2^{rac}\ X_2]$ (**2**), $[Cu_2L_2^{RR}\ X_2]$ (**2′**), $[Cu_2L_2^{SS}\ X_2]$ (**2″**), and $[Zn_2L_1^{rac}X_2]$ (**3**), $[Zn_2L_1^{RR}\ X_2]$ (**3′**), $[Zn_2L_1^{SS}\ X_2]$ (**3″**), $[Zn_2L_2^{rac}\ X_2]$ (**4**), $[Zn_2L_2^{RR}\ X_2]$ (**4′**), $[Zn_2L_2^{SS}\ X_2]$ (**4″**) were synthesized. Here the X represents either acetate or chloride ions and L_1 and L_2 are two different Schiff base ligands of 4-methyl-2,6-diformylphenol and 4-*tert*-butyl-2,6-diformylphenol, respectively, synthesized by treating *rac*-, (*R*)-(+)-, or (*S*)-(−)-1,1′-BNDA. Among these, complexes **1**−**4** are racemic containing L_1^{rac} and L_2^{rac} ligands, but the complexes **1′**−**4′** of L_1^{RR}, L_2^{RR} and **1″**−**4″** of L_1^{SS}, L_2^{SS} ligands are enantiopure in nature. All these complexes are obtained by the one-pot subcomponent approach as described in the Experimental Section and Scheme 1. A representative MS spectrum (Figure 1) for $[Zn_2L_1^{rac}(OAc)_2]$ (**3**) depicting a single dominant peak at *m*/*z* =

DOI: 10.1021/acs.inorgchem.8b03643
Inorg. Chem. XXXX, XXX, XXX−XXX

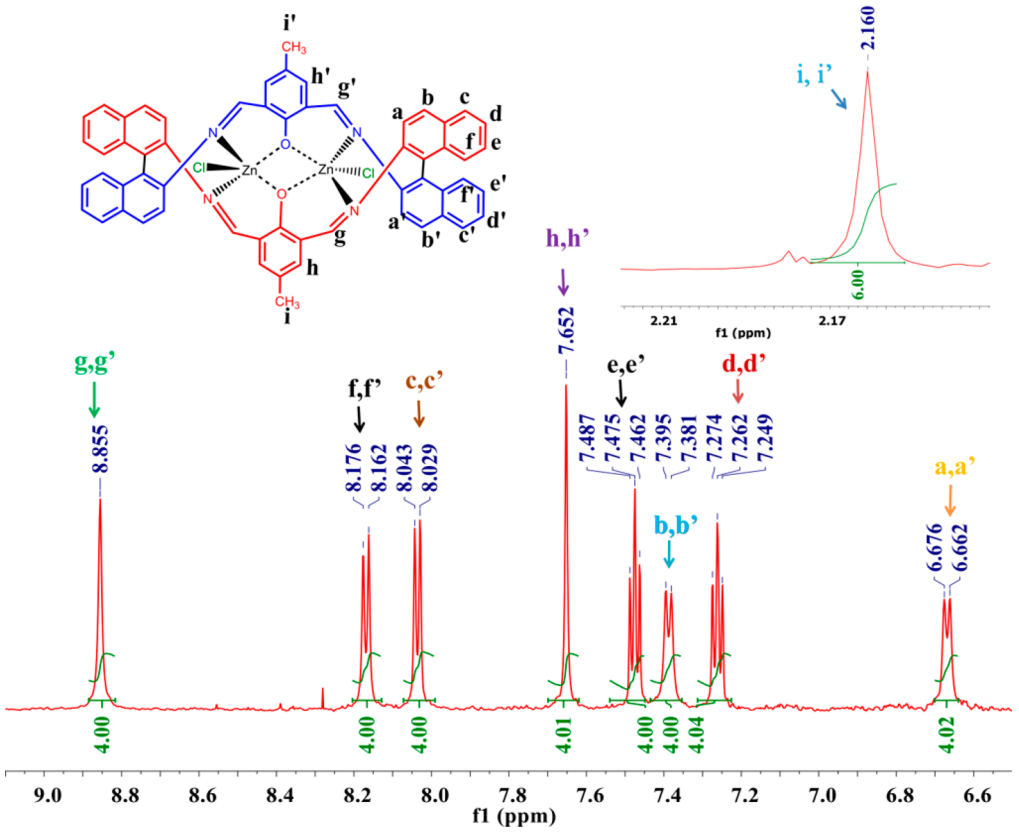

Figure 2. ^{1}H NMR $[Zn_2L_1{}^{SS}Cl_2]$ or $[3''.Cl_2]$ recorded in DMSO-d_6.

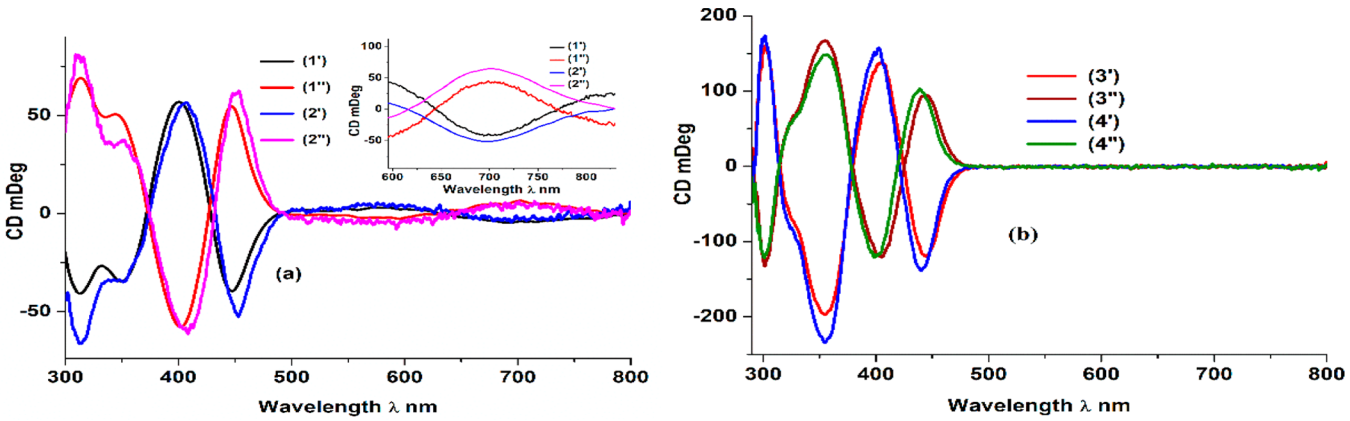

Figure 3. (a) CD spectra of $[Cu_2L_1{}^{RR}(OAc)_2]$ **1′**, $[Cu_2L_2{}^{RR}(OAc)_2]$ **2′** and their enantiomeric counterparts (**1″**, **2″**) recorded in THF (1×10^{-4} M). The insets show the d−d band (1×10^{-3} M). (b) CD spectra of zinc complexes were recorded in THF (1×10^{-4} M).

1011.34 along with isotopic peaks matches the calculated value 1011.17 of the monocationic species $[\mathbf{3}\text{-}(OAc)]^+$ or $[Zn_2L_1{}^{rac}(OAc)]^+$. The positive ion ESI-MS of all the helicates, depicting monocationic species $[M_2L(OAc)]^+$ in common, confirms the formation of binuclear neutral complexes (Figures S1−S12).

IR spectra of the complexes reveal the characteristic OH, C═N stretching frequencies at 3433 ± 5 and 1629 ± 5 cm^{-1} (Figure S13 and Figure S14). Both ^{1}H and ^{13}C NMR of zinc(II) dimers substantiate the formation of respective complexes (Figure S5). The ^{1}H NMR spectra of all zinc helicates **3**−**3″** and **4**−**4″** (Figure S15−S29), depicting a singlet at δ = 8.6−8.8 ppm in both, corresponding to four hydrogens, confirm the existence of the azomethine peak (CH═N); a set of multiplets in the region δ = 6.75−8.50 ppm correspond to an integral ratio of 28 hydrogens asserting the aromatic protons. Similarly, the singlet at 2.06−2.16 ppm corresponding to 3H of CH_3 of aromatic substitution is observed for **3**−**3″** complexes (Figures S15−S22), and a similar singlet at 1.20−1.25 ppm corresponding to 18 hydrogens of $-C(CH_3)_3$ from **4**−**4″** (Figures S23−S28) matches the respective complex. A representative ^{1}H NMR spectrum of $[Zn_2L_1{}^{SS}Cl_2]$ (**3″**) is shown in Figure 2.

Electronic spectra of the complexes (Figure S6) have shown similar spectral patterns. The ligand centered bands at approximately 264−270 and 285−290 nm are attributed to the σ−π^* and π−π^* transitions. The peak at 421−431 nm revealed the LMCT transition caused by the phenolate oxygen

DOI: 10.1021/acs.inorgchem.8b03643
Inorg. Chem. XXXX, XXX, XXX−XXX

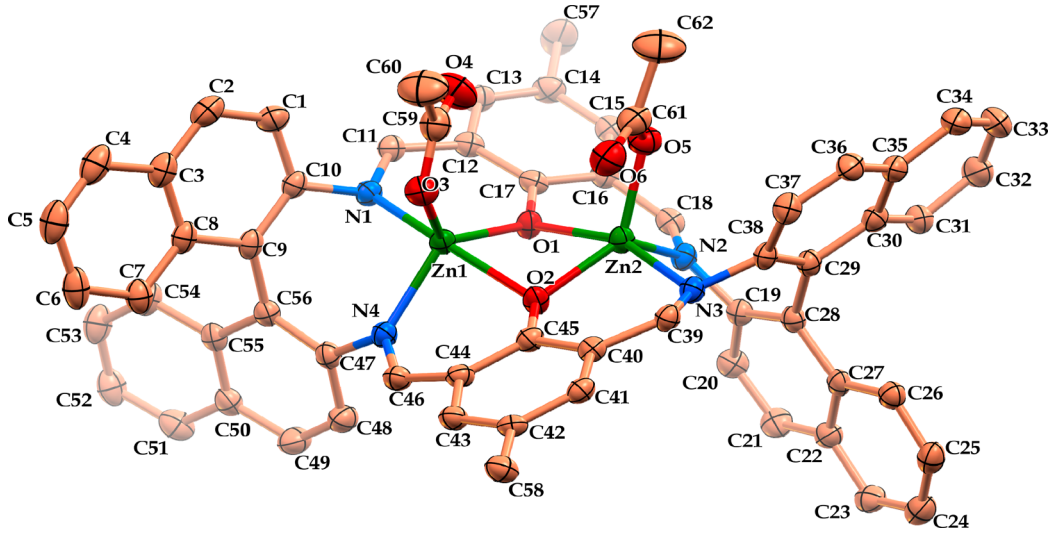

Figure 4. Thermal ellipsoid plot depicting the neutral dimeric $[Zn_2L_1^{rac}(OAc)_2]$ **3** with atom numbering scheme (45% probability factor for the thermal ellipsoids; lattice water, acetonitrile, and hydrogen atoms are omitted for clarity).

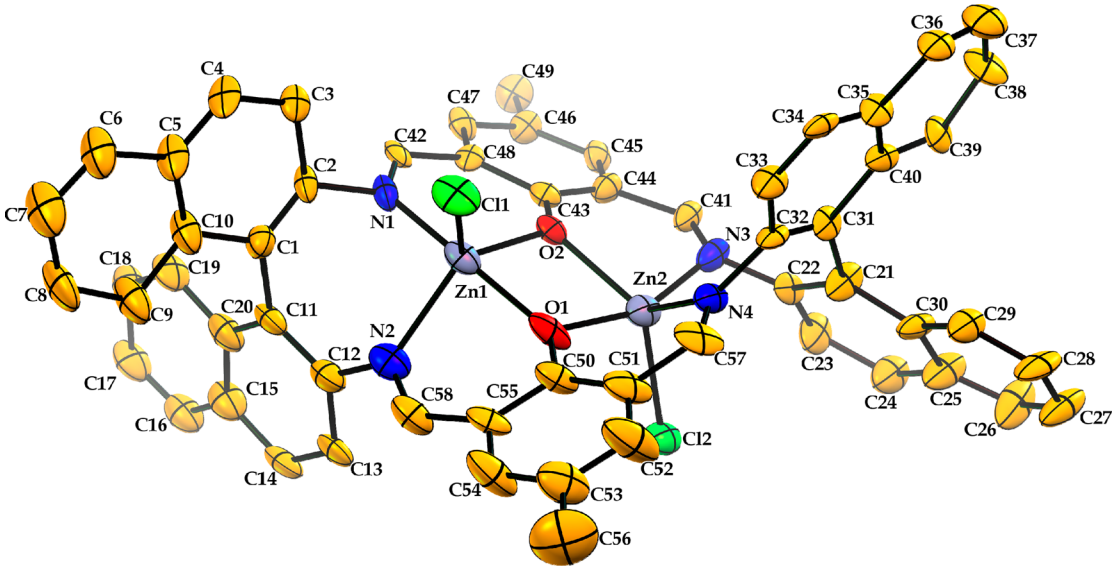

Figure 5. Thermal ellipsoid plot depicting the neutral dimeric $[Zn_2L_1^{SS}Cl_2]$ or $[3''.Cl_2]$ complex with atom numbering scheme (45% probability factor for the thermal ellipsoids; lattice water, acetonitrile, and hydrogen atoms are omitted for clarity).

to Cu(II) and Zn(II) center. Further, the position of the d−d band at 660−670 nm in all the copper(II) helicates revealed a pentacoordinated square pyramidal geometry of Cu(II) (Figures S30 and S31).

The CD spectra (Figure 3a) of the Cu(II) complexes **1′**, **2′** against **1″**, **2″** depicting exactly opposite Cotton effects; it is obvious that the complexes are enantiopure. In addition, the opposite optical sign in their d−d band (600−800 nm) in Figure 3 representing the metal-centered chirality suggests ΛΛ in $Cu_2L_1^{RR}$ (of **1′**), $Cu_2L_2^{RR}$ (of **2′**) and ΔΔ chirality in $Cu_2L_1^{SS}$ (of **1″**), $Cu_2L_2^{SS}$ (of **2″**). To understand its chiral stability, the effects of temperature and solvent were investigated by adapting a representative complex **3′** and changing the temperature in the range −10 to 60 °C using the CD spectral technique. This systematic study indicates that the complexes are chirally stable in the studied temperature range (Figure S32a). Similarly, the CD spectra recorded in different solvents such as DMSO, THF, methanol, dichloromethane, and chloroform have also shown no change in their CD pattern illustrating that the solvents did not show any change in Cotton effect (Figure S32b). The CD and optical rotatory dispersion (ORDE) in combination (Figure S8) confirm that the $Cu_2L_1^{RR}$ exhibit negative cotton (ΛΛ) effect (Figure S33), while $Cu_2L_1^{SS}$ exhibit positive cotton (ΔΔ) effect (Figure S34).

The complex $[Zn_2L_1^{rac}(OAc)_2]$ **3** was crystallized out by slow evaporation from its acetonitrile solution, which yielded crystals of yellow color suitable for X-ray analysis (Figure S9). Complex **3**, resolved in the monoclinic system with $P2_1/n$ space group, is composed of two Zn(II) atoms (Zn1 and Zn2), one binaphthyl macrocyclic helically twisted ligand L_1, two coordinated acetate anions, one water molecule, and an acetonitrile located as a solvent of crystallization in the lattice. As depicted in Figure 4, both Zn atoms in the complex are placed within the terminally closed helical ring and possesses a N_2O_3 penta-coordination. In the dimeric unit, the ZnN_2O_3

DOI: 10.1021/acs.inorgchem.8b03643
Inorg. Chem. XXXX, XXX, XXX−XXX

Scheme 2. Self-Sorting Phenomena of Axially Chiral BNDA in Racemic and Enantiopure *S*-(−) and *R*-(+)-BNDA [M = Cu^{2+}, Zn^{2+}, X = OAc^-, Cl^-, L = L_1 or L_2]

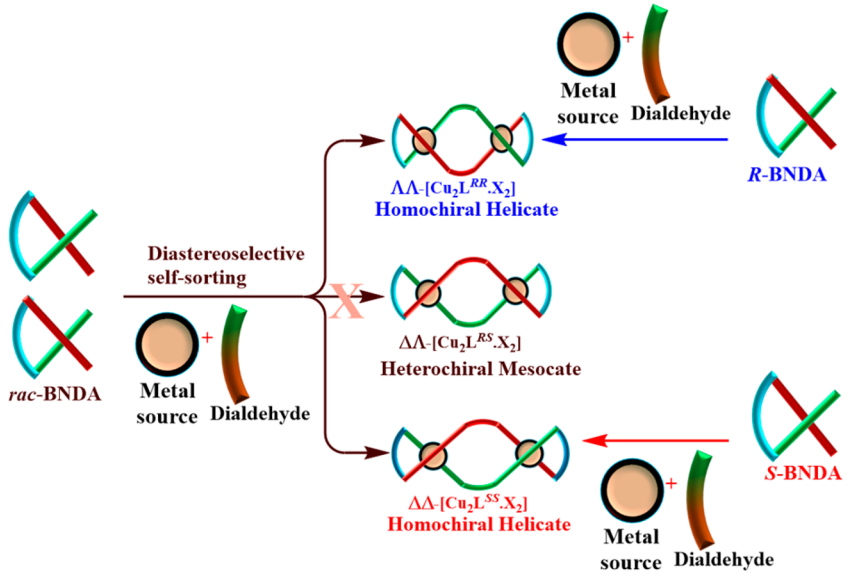

core of each metal center has distorted square pyramidal geometry. The dinuclear and non-centrosymmetric structure of **3** (Figure 5) has thus constructed a $Zn_2N_4O_2$ core. The hexadentate macrocyclic ligand with N_4O_2 donor set shows a helical twist upon coordination with two Zn(II) ions. Each Zn(II) ion coordinating with two azomethine nitrogen is further bridged by two phenolate oxygen atoms via μ_2-bridge. The distorted square pyramidal geometry is completed by monodentate coordination of O atom of the acetate anion with a tetrahedral bias (Zn1−O3 = 1.937(2) and Zn2−O5 = 1.954(2) Å) formed by the N_2O_2 core. The basal planes of both metal centers are provided by two imino nitrogens and two phenoxy bridging oxygens with Zn−N distances Zn(1)−N(4) = 2.051(2), Zn(1)−N(1) = 2.082(2), and Zn(2)−N(2) = 2.070(2), Zn(2)−N(3) = 2.104(2) Å. Intermetallic Zn(1)···Zn(2) distance within the dimer is calculated as 3.1056(5) Å with Zn(1)−O(1)−Zn(2) and Zn(1)−O(2)−Zn(2) angles 98.12(7)° and 98.13(4)°. In the dimeric complex *rac*-$[Zn_2L_1]$ **3**, the dihedral angles between the naphthyl-benzylideneamine moieties coordinating to the respective metal centers as well as between binaphthyl units of the ligand have shown differences. Thus, the dihedral angle between the *N*-naphthyl-benzylideneamine moiety (i.e., between C1 to C10−N1−C11 and C46 to C47−N4−C56) is 74.91°, while between the binaphthyl units (i.e., C1 to C10 and C47 to C56), it is 70.48°. The dihedral angles in the Zn2 geometry, between the *N*-naphthyl-benzylideneamine moiety (i.e.,C19 to C28−N2−C18 and C29 to C38−N3−C39) as well as between the binaphthyl units (i.e., C19 to C28 and C29 to C38), are ∼86° and remain almost perpendicular to make effective coordination with the respective metal atoms. Interestingly, the apical coordination of the square pyramidal geometry on each Zn(II) in the dimeric unit is occupied by acetate anions. It is noteworthy to mention that both acetate ions reside on the same side in the racemic complex, and hence the opposite sites of the basal plane are free. Possessing four molecules in the unit cell, the structure analysis suggests that two are in ΔΔ form, while the other two are in ΛΛ form reflecting their homochiral dimers in the racemic complex, i.e., $[\Lambda\Lambda\text{-}(Zn_2L_1{}^{RR}(OAc)_2]$ and $[\Delta\Delta\text{-}(Zn_2L_1{}^{SS}(OAc)_2]$. The single crystal analysis of the racemic complex did not show any heterochiral dimer $\Lambda\Delta\text{-}[(Zn_2L_1{}^{RS}(OAc)_2]$ formation, although it was expected.[19] Thus, the R and S−BNDA moieties follow the spontaneous separation in the dimeric complexation. Thus, the helical conformation favors the formation of self-sorting behavior and promotes the formation of ΛΛ and ΔΔ homochiral pairs instead of a heterochiral ΔΛ pair.

The helicate $[\mathbf{Zn_2L_1{}^{SS}Cl_2}]$ synthesized with enantiopure $\mathbf{L_1{}^{SS}}$ has given a suitable single crystal by slow evaporation of its acetonitrile solution at room temperature. The structure was resolved in the monoclinic crystal system with chiral space group C_2 with five acetonitrile molecules in the lattice. The crystal structure $[\mathbf{3''.Cl_2}]$ illustrates that the ligand L^{SS} in the complex exists in helical chirality *M*, with metal centered homochiral component ΔΔ. Possessing almost identical dimeric units, the difference between these two structures of **3** and **3″** lies mainly on their chirality. Each Zn(II) atoms in the dimeric unit possess a square pyramidal geometry and are nonsuperimposable on each other. The Zn1 with N_2O_2Cl chromophores are assembled in a square pyramidal geometry. The basal plane formed by N_2O_2 exhibits coordination with two azomethine nitrogens [Zn1−N1 = 2.021(17), Zn1−N2 = 2.137(19) Å] and two phenolate oxygens [Zn1−O1 = 1.94(2), Zn1−O2 = 2.021(17)Å].

In a similar square base constructed by O1O2N3N4 with Zn2 atom, the chloride ion Cl2 fulfilling the fifth site completes a distorted square pyramidal geometry. Thus, both Zn(II) atoms in the dimeric unit form a square base with the N_2O_2 chromosphere; the fifth site on the square pyramidal geometry [Zn1−Cl1 = 2.266(5) and Zn2−Cl2 = 2.291(6)] is filled with chloride ions. The respective geometries are inverting to each other and are assembled in nonsuperimposable mirror images (Δ, Δ). The Zn(II) atoms within the dimeric unit are separated by a distance Zn1−Zn2 = 3.273 Å. The coordinatively unsaturated sixth site in each zinc(II) center is expected to play a crucial role in the asymmetric catalysis. Selected bond distance and bond angles for both complexes of $[\mathbf{3.(OAc)_2}]$ and $[\mathbf{3''.Cl_2}]$ are given in Table S1.

The racemic (*RS*) and enantiopure (*RR*, *SS*)-BNDA moieties in the ligands L_1 and L_2 of the dimeric formulation,

DOI: 10.1021/acs.inorgchem.8b03643
Inorg. Chem. XXXX, XXX, XXX−XXX

thus resulting in L_1^{rac}, L_2^{rac}, L_1^{RR}, L_2^{RR}, L_1^{SS}, and L_2^{SS} ligands, the self-assembly process followed in these respective complexation inspired us to derive the self-sorting pathway based on their chiroptical property. In general, helicates are intrinsically chiral and exist as a diastereomeric mixture of homochiral pairs (ΔΔ and ΛΛ)[21] and heterochiral mesocate ΔΛ[21] in the case of achiral helicands. The homochiral pairs in the mixtures thus possessing opposite chirality (ΔΔ and ΛΛ) cancel each other, and hence the net CD activity is nullified. In the present case, the racemic *R* and *S*−BNDA upon complexation follow a very interesting pathway as illustrated in Scheme 2. The *rac*-BNDA in L^{rac} have assembled in $[M_2L^{RR}.X_2]$ and $[M_2L^{SS}.X_2]$ mixtures in which the *R* and *S* enantiomers are equally separated into homochiral pairs constituting ΔΔ and ΛΛ chiral molecules in the unit cell as represented in eq 1. In the other case, using enantiopure *R*-BNDA and *S*-BNDA in complexes **1′−4′** and **1″−4″** results in self-assembly into $[M_2L_1^{RR}.X_2]$, $[M_2L_2^{RR}.X_2]$ and $[M_2L_1^{SS}.X_2]$, $[M_2L_2^{SS}.X_2]$ in their respective complexes as shown in eqs 2 and 3. On the other hand, the racemic ligands generally lead to the formation of heterochiral complex (ΔΛ) and/or mixture of homochiral pairs (ΔΔ and ΛΛ).[22,23] Generally, racemic ligands are known to produce diastereomeric mixtures.[20] Interestingly the present complex of L^{rac} produces only homochiral dimers instead of a diastereomeric mixture. This unique observation in the present complexes can be explained by self-sorting (self/nonself) behavior in the present chiral source of the ligands.[24] The axially chiral[25] BNDA in its different chiral forms, i.e., *R*-(+), *S*-(−), and racemic, particularly exhibits this unique self-sorting behavior. The BNDA in the racemic complexes **1−4** are self-assembled and produce homochiral helicates (ΔΔ and ΛΛ) during complexation and did not show the formation of any heterochiral mesocate (ΔΛ) as shown in eq 1. However, by incorporating enantiopure helicands, one can produce either one enantiopure ΔΔ or ΛΛ helicates.[26,27]

$$4MX_2 + L^{rac} \rightarrow \Lambda\Lambda\text{-}[M_2L^{RR}X_2] + \Delta\Delta\text{-}[M_2L^{SS}X_2] + 2X_2 \quad (1)$$

where L^{rac} = 50% ratio of *R* and *S*-BNDA.

$$2MX_2 + L^{RR} \rightarrow \Lambda\Lambda\text{-}[M_2L^{RR}X_2] + X_2 \quad (2)$$

$$2MX_2 + L^{SS} \rightarrow \Delta\Delta\text{-}[M_2L^{SS}X_2] + X_2 \quad (3)$$

Having used enantiopure *R*, *S* and *rac*-BNDA in the ligand construction, the selective formation of optical isomers in the dinuclear complexation was analyzed based on the single crystal X-ray structure, circular dichroic cotton activity, and UFLC (ultrafast liquid chromatography) results. The crystal structure of $[Zn_2L_1^{rac}(OAc)_2]$ **3** illustrates that the unit cell contains a pair of homochiral helicates $[Zn_2L_1^{RR}(OAc)_2]$ and $[Zn_2L_1^{SS}(OAc)_2]$ in which the metal centered chirality exists in homochiral ΛΛ and ΔΔ forms. The unit cell contains four molecules, two representing *P*-helicates with ΛΛ component, and the other two *M*-helicate in the ΔΔ form. Thus, the self-sorting behavior of this racemic ligand in $[Zn_2L_1^{rac}(OAc)_2]$ **3** leads to formation of two pairs of molecules, i.e., a pair of (*P*)-ΛΛ-$[Zn_2L_1^{RR}(OAc)_2]$ and a pair of (*M*)-ΔΔ-$[Zn_2L_1^{SS}(OAc)_2]$ in the unit cell (Figure S35) as shown in eq 1. The crystal structure analysis thus rules out the formation of heterochiral ΛΔ-$[Zn_2L_1^{RS}(OAc)_2]$ mesocate. However, the use of L^{SS} in the complex **3″** selectively leads to formation of enantiopure ΔΔ-$[Zn_2L_1^{SS}.Cl_2]$ (Figure S36). The single crystal X-ray analysis in **3″** suggesting the chiral space group further augments the existence of chirality with flack parameter value 0.05(2). As expected, the racemic helicates with 50:50% ratio of enantiomers nullify the chiral contribution in CD spectra and give a flat line.

In the UFLC, using phenomenox lux cellulose-1 column and isopropyl alcohol/*n*-hexane (10/90%, 1 mL/min) as a mobile phase, the enantiopure complexes are eluted as a single peak suggesting that they are 100% *ee* (Figures S10, S37). When the racemic helicates **1−4** were eluted, all of them have showed two independent peaks corresponding to opposite enantiomers. We did not find any third peak in the chromatogram corresponding to mesocate confirming the absence of heterochiral mesocate (ΔΛ). Thus, the chromatogram giving only two separate peaks corresponds to ΛΛ and ΔΔ homochiral compounds, supporting the observation in the crystal structure of the racemic complex $[\mathbf{3}.(\mathbf{OAc})_2]$. The absence of the third peak thus obviously concludes the absence of mesocate ΔΛ. This observation further supports that the $[M_2L_1^{RR}.X_2].[M_2L_1^{SS}.X_2]$ homochiral pairs lead to CD absence; thus, ruling out the formation of heterochiral $[M_2L_1^{RS}.X_2]$ in **1−4** is noteworthy. This gives an understanding that the racemic complex **1−4** generates ΛΛ and ΔΔ homochiral dimers, but the respective enantiopure complexes **1′−4′** generate purely ΛΛ-$[M_2L^{RR}X_2]$, while **1″−4″** produce only ΔΔ-$[M_2L^{SS}X_2]$ dinuclear complex selectively.

Among the 12 complexes shown in Scheme 1, eight (**1′−4′** and **1″−4″**) are enantiopure, while the remaining four (**1−4**) are racemic. The detailed chiroptical study on these enantiopure complexes has inspired us to investigate them on enantioselective catalysis. Mesohydrobenzoin containing two hydroxyl groups is known for its C_2 symmetry. Benzoylation of both hydroxyl groups is an easy task, but the selective benzoylation of one of these two symmetric hydroxyls of this mesodiol is of significant importance. Understanding the challenge involved in the reaction, we have adapted these complexes as catalysts to obtain enantiorich monobenzoylated products and the results are summarized in Table 1. Accordingly, the mesohydrobenzoin (5a) to monobenzoylation (5b) reaction was performed. Initially, the blank reaction performed without catalyst provides a moderate conversion without any enantioselectivity (Table 1, entry 1). Then, all eight chiral catalysts were screened with 5 mol % catalyst loading, using 2 equiv DIPEA (*N*,*N*-diisopropylethylamine), benzoyl chloride (PhCOCl, 1 equiv), and chloroform as solvent at RT. By adapting racemic complexes **1−4** as a catalysts, the respective products (5b) are found to be racemic as expected. Hence, by replacing the racemic complex with respective enantiopure complexes **1′−4′** and **1″−4″**, the respective data are presented in Table 1 (entries 2−9). Compared to the Cu catalysts (**1′**, **1″**, **2′**, **2″**) (Table 1, entries 2−5), the Zn(II) catalysts **3′**, **3″**, **4′**, **4″** (Table 1, entries 6−9) generated better yield (92%) and enantioselectivity (78%), with shorter reaction time (10 h). Thus identifying the zinc(II) helicate as a suitable catalyst, we have optimized the reaction conditions below.

In our attempt to optimize the catalyst loading, we varied the amount of catalyst from 0.5 to 10 mol % (Table 1, entries 10−16) and found 2 mol % of catalyst giving the highest yield (92%) and enantioselectivity (85%) of monoester (Table 1, entry 12).

As the solvent is known to play an important role, we next performed a systematic screening of different solvents. Considering the earlier reports, the main emphasis was given

DOI: 10.1021/acs.inorgchem.8b03643
Inorg. Chem. XXXX, XXX, XXX−XXX

Table 1. Screening of Catalyst[a]

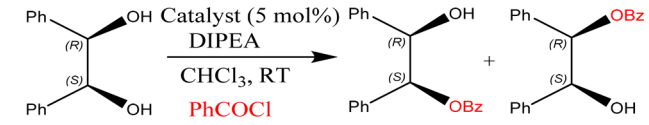

entry	catalyst	catalyst loading (mol %)	yield[b] %	*ee*[c] %(configuration)
1	blank	---	55	---
2	**1′**	5	88	69(1*S*,2*R*)
3	**1″**	5	85	68(1*S*,2*R*)
4	**2′**	5	89	67(1*S*,2*R*)
5	**2″**	5	87	67(1*R*,2*S*)
6	**3′**	5	92	78(1*S*,2*R*)
7	**3″**	5	91	78(1*R*,2*S*)
8	**4′**	5	90	77(1*S*,2*R*)
9	**4″**	5	90	77(1*R*,2*S*)
10	**3′**	0.5	90	51(1*S*,2*R*)
11	**3′**	1	92	62(1*S*,2*R*)
12	**3′**	2	92	85(1*S*,2*R*)
13	**3′**	4	90	78(1*S*,2*R*)
14	**3′**	6	91	70(1*S*,2*R*)
15	**3′**	8	90	68(1*S*,2*R*)
16	**3′**	10	89	62(1*S*,2*R*)

[a]All the reactions were carried out with 0.2 mmol of mesohydrobenzoin, 0.2 mmol of PhCOCl, 0.4 mmol of DIPEA, and 2 mL of solvent was used. [b]Isolated yield. [c]Determined by UFLC (Lux cellulose-1 column). The reaction time for the Cu_2-complex is 12 h and Zn_2 is 10 h.

to halogenated solvents (Table 2, entries 1−3). Hence, a series of halogenated solvents like dichloroethane, dichloromethane, and carbon tetrachloride along with some nonhalogenated solvents (Table 2, entries 4−6) like tetrahydrofuran, ethyl acetate, and toluene (Table 2, entry 6) were tested. Among these, DCM was found to give good yield, 96%, and better enantioselectivity, 88% (Table 2, entry 2). For further increase in the yield and enantioselectivity, the reaction temperature was optimized by varying temperature such as 40, 20, 10, 0, −5, and −10 °C (Table 2, entries 7−12). The highest yield, 98%, and enantioselectivity, 92%, at 0 °C prompted us to fix this as optimized temperature. In a search to identify a suitable base, various bases (Table 2, entries 13−16) such as triethylamine, lutidine, sodium carbonate, and potassium carbonate were tested. With the results being inferior compared to DIPEA, all the follow-up reactions are conducted using DIPEA as base.

Table 2. Screening of Reaction Condition[a]

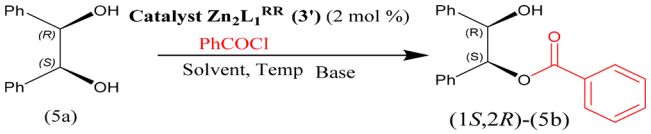

entry	base	solvent	temp (°C)	yield[b] %	*ee*[c] %
1	DIPEA	$CH_3CH_2Cl_2$	RT	90	75
2	DIPEA	CH_2Cl_2	RT	96	88
3	DIPEA	CCl_4	RT	85	76
4	DIPEA	THF	RT	84	70
5	DIPEA	EtOAc	RT	87	67
6	DIPEA	Toluene	RT	80	78
7	DIPEA	CH_2Cl_2	40	92	75
8	DIPEA	CH_2Cl_2	20	96	88
9	DIPEA	CH_2Cl_2	10	96	88
10	DIPEA	CH_2Cl_2	0	98	92
11	DIPEA	CH_2Cl_2	−5	88	88
12	DIPEA	CH_2Cl_2	−10	85	85
13	Et_3N	CH_2Cl_2	0	89	78
14	lutidine	CH_2Cl_2	0	87	76
15	Na_2CO_3	CH_2Cl_2	0	95	70
16	K_2CO_3	CH_2Cl_2	0	95	75

[a]All the reactions were carried out with 2 mol % of catalyst, 0.2 mmol of mesohydrobenzoin, 0.2 mmol of PhCOCl, 0.4 mmol of base, and 2 mL of solvent. [b]Isolated yield. [c]Determined by UFLC (Lux cellulose-1 column). The reaction time for entries 1−9 is 10 h and for the rest is 8 h.

Adapting the reaction conditions optimized above, we further explored varying substrates of meso-1,2-diols (Table 3, 5b−15b) catalyzed by both **3′** and **4′**. In the case of hydrobenzoin (5a) both of them are behaving very similarly (Table 3, 5b), i.e., 98% and 97% yield and 92% and 90% *ee* (**3′** and **4′**, respectively). The substrate 2,3-butanediol (6a), which possess an additional methyl group, gives good yield 96% and 95%, but differs by its poor *ee*, i.e., 40% and 22% (Table 3, 6b). Then, we moved from acyclic diol to cyclic diol substrates containing five-membered, six-membered, and eight-membered rings. Although this attempt did not give encouraging *ee*, the cyclopentane diol (7a) has converted to monobenzoylated product (7b) with 97% yield and 44% and 35% *ee* (Table 3, 7b). Similarly, the monoester 8b obtained from cyclohexane diol (8a), both catalysts **3′** and **4′** produce yield of 95% but differ in their *ee* as 70% and 31% (Table 3, 8b). Finally, the cyclooctane diol (9a) gives 94% and 95% yield and 30% and 42% *ee* of monoester product (9b) (Table 3, 9b). From this substrate variation, we conclude that the phenyl substituted 1,2-diol (5a) only gave the best result (Table 3, 5b). A strong $\pi-\pi$ interaction between the phenyl moiety of substrate mesodiol[28] and the aromatic rings on the BNDA of the catalyst might have influenced this enhanced activity.

It is noteworthy to mention that the catalysts **3′** and **4′** favored the desymmetrization of 1,2-diphenyl substituted diols over the cyclic substrates. The lack of $\pi-\pi$ interaction between all other substrates, resulting in less *ee*, is obvious to understand. Thus, with the $\pi-\pi$ interaction playing the crucial role, the $P(\Lambda\Lambda)$ stereostructure in $[\mathbf{Zn_2L_1}^{RR}]$ **3′** promotes (1*S*,2*R*) products, while $M(\Delta\Delta)$ stereostructure in $[\mathbf{Zn_2L_1}^{SS}]$ **3″** promotes (1*R*,2*S*) enantiomeric product. Hence by keeping mesohydrobenzoin as a choice of substrate, various aroyl, cyclic, and acyclic acyl chlorides were treated with acylating agent under the above optimized reaction conditions using **3′** as a catalyst (Table 3, 10b−15b). Consequently, various electron donating and electron withdrawing substituted benzoyl chlorides were tested. When 4-fluorobenzoyl chloride (10a) was used, the corresponding monoester (10b) was produced with 96% yield and 82% *ee* (Table 3, 10b). The 4-nitrobenzoyl chloride (11a) gives monoester (11b) with 95% yield, but the enantioselectivity was reduced to 10% (Table 3, 11b). In the case of 11b, the low *ee* might have been obtained, because of the steric hindrance of the bulky nitro group at the fourth position. The remaining 4-methylbenzoyl chloride (12a) and 2-fluorobenzoyl chloride (13a) gives monoester (12b and 13b) with good yield, 95% and 93%, respectively and *ee* 88% and 78% (Table 3, 12b and 13b). Since the aroyl chlorides are giving encouraging results, we also screened some

DOI: 10.1021/acs.inorgchem.8b03643
Inorg. Chem. XXXX, XXX, XXX−XXX

Table 3. Asymmetric Benzoylation of Meso-1,2-diols[a]

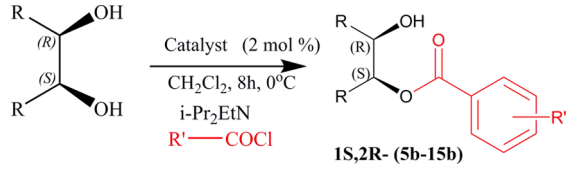

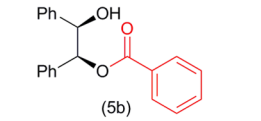
(5b)
R'=Benzoylchloride
$Zn_2L_1^{RR}$ = Yield 98%, ee = 92%
$Zn_2L_2^{RR}$ = Yield 97%, ee = 90%

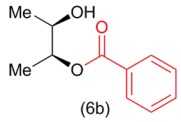
(6b)
R'=Benzoylchloride
$Zn_2L_1^{RR}$ = Yield 96%, ee =40%
$Zn_2L_2^{RR}$ = Yield 95%, ee = 22%

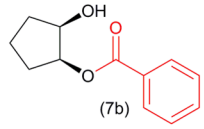
(7b)
R'=Benzoylchloride
$Zn_2L_1^{RR}$ = Yield 97%, ee =44%
$Zn_2L_2^{RR}$ = Yield 97%, ee = 35%

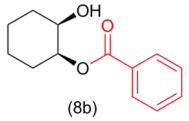
(8b)
R'=Benzoylchloride
$Zn_2L_1^{RR}$ = Yield 95%, ee = 70%
$Zn_2L_2^{RR}$ = Yield 95%, ee = 31%

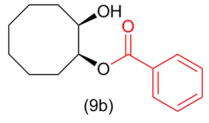
(9b)
R'=Benzoylchloride
$Zn_2L_1^{RR}$ = Yield 94%, ee =30%
$Zn_2L_2^{RR}$ = Yield 95%, ee = 42%

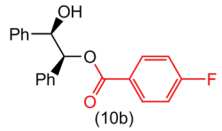
(10b)
R'=4-F-benzoylchloride
$Zn_2L_1^{RR}$ = Yield 96%, ee = 82 %

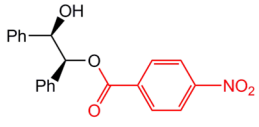
(11b)
R'=4-NO_2-benzoylchloride
$Zn_2L_1^{RR}$ = Yield 95%, ee =10%

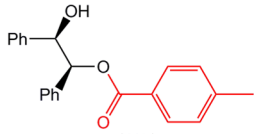
(12b)
R'=4-CH_3-benzoylchloride
$Zn_2L_1^{RR}$ = Yield 95%, ee = 88%

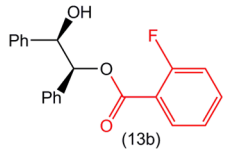
(13b)
R'=2-F-benzoylchloride
$Zn_2L_1^{RR}$ = Yield 93%, ee = 78%

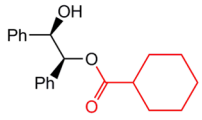
(14b)
R'= Cyclohexanecarbonyl chloride
$Zn_2L_1^{RR}$ = Yield 94%, ee = 34%

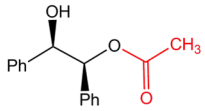
(15b)
R'= Acetyl chloride
$Zn_2L_1^{RR}$ = Yield 96%, ee = 18%

[a]All the reactions were carried out with 2 mol % of catalyst, and 0.2 mmol of mesohydrobenzoin, 0.2 mmol of PhCOCl, 0.4 mmol of DIPEA, and 2 mL of solvent were used. Yields presented here are isolated yields, and *ee* values were determined by UFLC (Lux cellulose-1 column).

nonaroyl cyclic (cyclohexanecarbonyl chloride, 14a) and acyclic acyl chloride (acetyl chloride, 15a) which produced monoesters (14b and 15b) with yield (94% and 96%, respectively) and *ee* (34% and 18%, respectively) (Table 3,14b and 15b). These two nonaroyl chlorides, although giving good yield, resulted in poor enantioselectivities. This detailed study suggests that the benzoyl chloride gives the best results (Table 3, 5b) among the acylating agents.

In an attempt to understand the mechanism involved in the catalytic process, based on the crystal structures of [**3.(OAc)$_2$**] and [**3′.Cl$_2$**], we propose the mechanism in Scheme 3. In the racemic crystal **3**, both acetate ions coordinated to Zn(II) metal centers reside on the same side. Hence, the diol is approaching the Zn(II) ions through the sixth vacant site by rearranging its geometry from square pyramidal to distorted octahedral. The intramolecular M−M distance derived from the crystal structure ranges 3.1−3.2 Å in the dimeric association, and the distance between the hydroxyl groups of the diol can comfortably make a six-membered chelate ring involving Zn1 and Zn2 from the same side. The Zn1−Zn2 distance, 3.10 Å, derived from the crystal structure **3** and the

Scheme 3. Tentative Model of the Substrate−Catalyst Interaction: (a) Racemic Complex; (b) Enantiopure Complexes

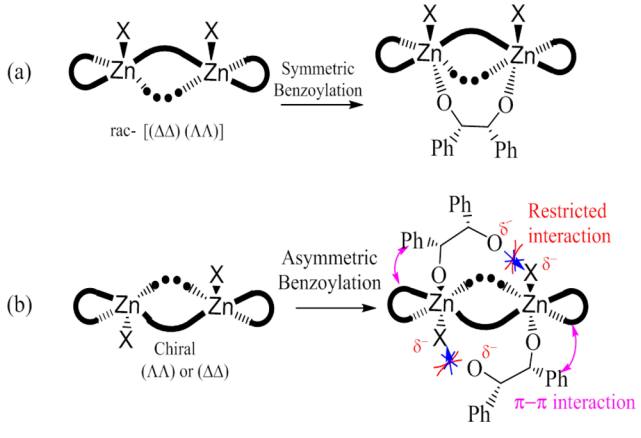

O···O distance in the hydrobenzoin[29] ranging 2.69−3.59 Å provide a strong possibility for chelate coordination involving

DOI: 10.1021/acs.inorgchem.8b03643
Inorg. Chem. XXXX, XXX, XXX−XXX

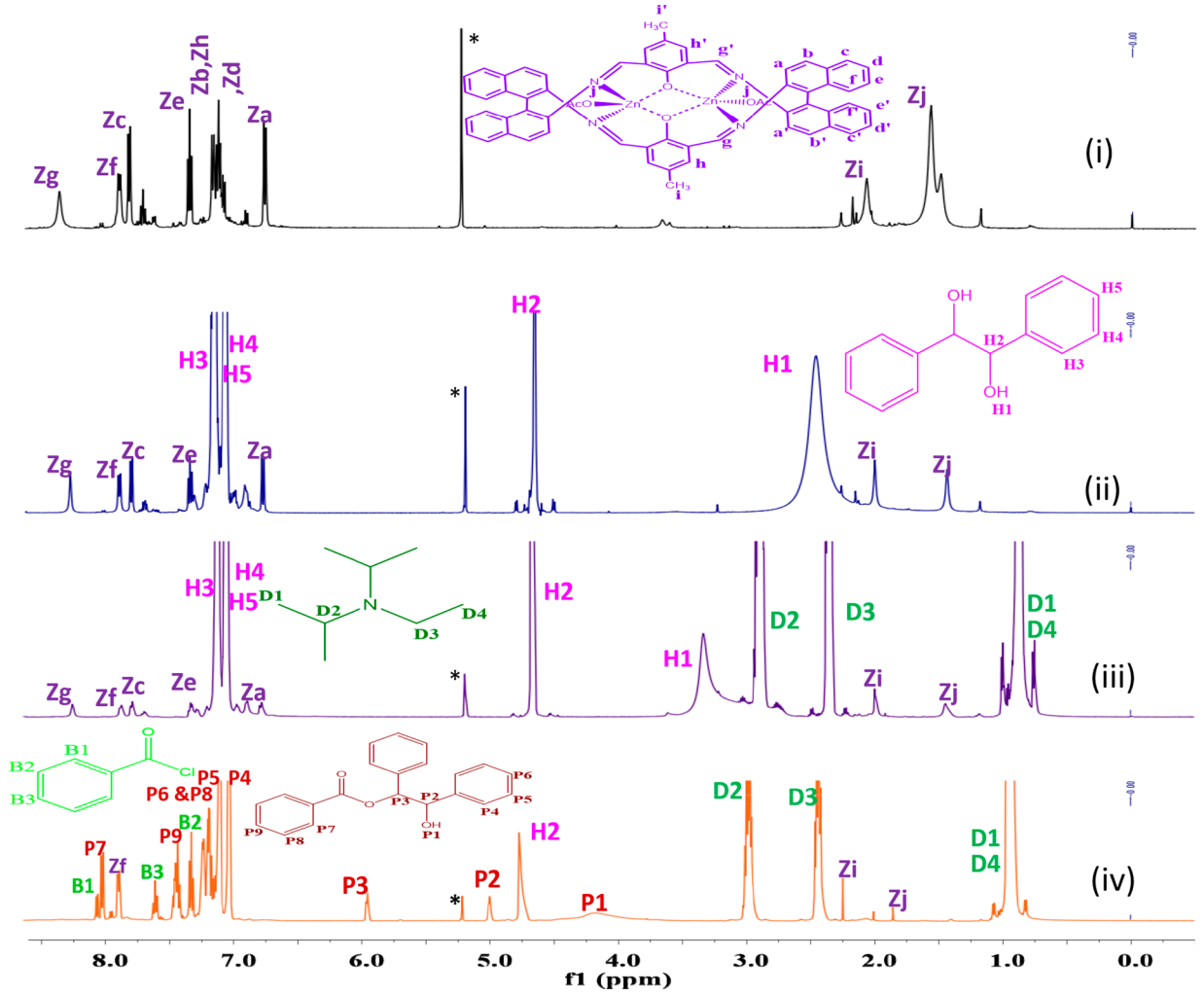

Figure 6. ^{1}H NMR for (i) [$\mathbf{Zn_2L_1}^{RR}$], (ii) addition of hydrobenzoin, (iii) addition of DIPEA, and (iv) addition of C_6H_5COCl. Here, Z − catalyst, H − Hydrobenzoin, D − DIPEA, B − Benzoyl Chloride, P − monoester product, * − solvent CH_2Cl_2.

(Zn−O−C−C−O−Zn) of the same zinc dimer. Thus, the diastereomeric dimers, i.e., ΛΛ and ΔΔ pairs in complex **3** might simultaneously promote the benzoylation on both the hydroxyl group of the mesodiols. As a result, racemic complex **3** failed to break the symmetry (Scheme 3a) of mesodiols. The *P*(ΛΛ) and *M*(ΔΔ) stereostructure of the chiral catalysts [**3′.OAc$_2$**] and [**3′.Cl$_2$**] in their enantiopure form accelerates the enantioselectivity. The *π*−*π* stacking interaction between the phenyl rings of the BNDA moiety on the catalysts and substrates in combination favors the enantioselective product (Scheme 3). The absence of such *π*−*π* stacking interaction in the case of nonaromatic cyclic (**6b**−**9b**) and acyclic products (**14b** and **15b**) failed to provide enantioselectivity and supports the significance of the aromatic ring in the catalysis. As shown in the crystal structure of the racemic complex **3**, both Zn(II) ions in the dimer projecting the apical site (Scheme 3a) on the same side exists as ΔΔ and ΛΛ. Thus, the stereostructure of catalyst **3** favors the substrate to approach through the vacant side, and hence both hydroxyl groups get equal opportunity for benzoylation, resulting in a symmetric benzoylation. Thus, in the case of a racemic catalyst, both the metal−metal distance and the geometry in the dimer favor symmetric benzoylation.

In contrast, in the chiral complexes [$\mathbf{Zn_2L_1}^{RR}\mathbf{Cl_2}$] and [$\mathbf{Zn_2L_1}^{SS}\mathbf{Cl_2}$], the geometry of Zn(II) exists either in ΛΛ or ΔΔ, respectively, in the dimer; the accessible vacant site for the substrate is available for only one hydroxyl group from each side (Scheme 3b). Hence the other hydroxyl of the diol remains unaffected, which favors the desymmetrization of the C_2 symmetric mesodiol.

To ascertain the mechanism in solution state, we have recorded a series of systematic ^{1}H NMR (Figure 6). Four different experiments such as (i) ^{1}H NMR for [$\mathbf{Zn_2L_1}^{RR}$], (ii) addition of hydrobenzoin, (iii) addition of DIPEA, and (iv) addition of C_6H_5COCl (here Z − catalyst, H − Hydrobenzoin, D − DIPEA, B − Benzoyl Chloride, P − monoester product) were carried out. The hydroxyl proton observed at δ = 2.46 ppm (H1) was found to shift to δ = 3.3 ppm upon adding DIPEA. Subsequently, a further shift to δ = 4.0 ppm was observed at the end of the catalytic run representing the hydroxyl in the product (**P1**), showing a broad resonance.

The CH proton H2 of the mesohydrobenzoin at δ = 4.7 ppm corresponded to two hydrogens giving a strong singlet, ensuring the existence of C_2 symmetry in Figure 6(ii). However, as the reaction progresses with benzoyl chloride, the simultaneous decrease in intensity of H2 and appearance of two new peaks at **P2** and **P3** at Figure 6(iv) illustrates the symmetry-breaking leading to desymmetrized monobenzoylated product formation.

DOI: 10.1021/acs.inorgchem.8b03643
Inorg. Chem. XXXX, XXX, XXX−XXX

Scheme 4. Proposed Mechanism for Desymmetrization of Mesodiol by [$Zn_2L_1^{RR}$] (3′) Catalyst

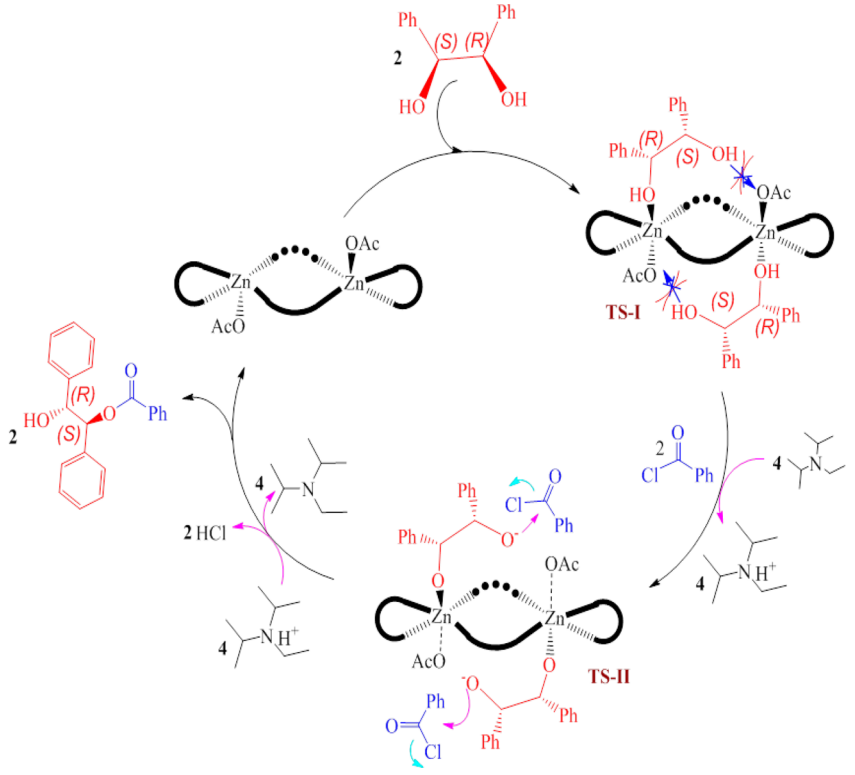

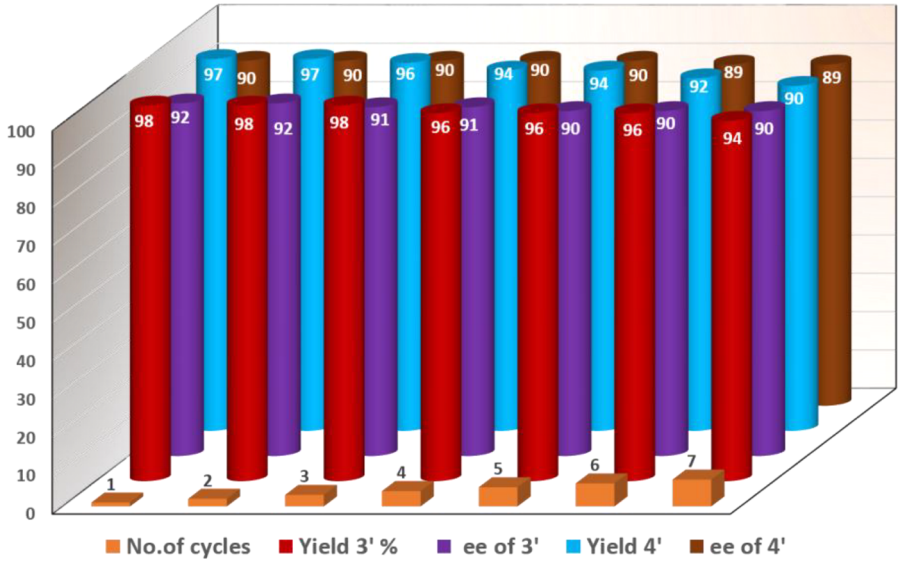

Figure 7. Recyclability of the catalyst **3′** and **4′** in mesohydrobenzoin with benzoyl chloride in an optimized condition.

Based on our understanding, we propose a probable mechanism for desymmetrization of mesodiol in Scheme 4. In the first step, the substrate interacts with the catalyst through the sixth vacant site of the Zn(II) center, leading to an octahedral geometry (TS-I). Then, the alcoholic protons of diol get deprotonated by DIPEA to form a diisopropylethylammonium ion. One of the two hydroxyl ions coordinates with one Zn(II), leaving the other hydroxyl ion free to interact with the carbonyl carbon of the benzoyl chloride as shown in TS-II. The nucleophilic addition between the carbonyl carbon of benzoyl chloride (Ph-$OC^{\delta+}$) and free hydroxyl ion of the diol combine to form a stereoselective monoester product leaving the chloride ion as hydrochloric acid. High stereoselectivity was observed only in mesohydrobenzoin compared to the other substrates. As stated above, the phenyl moiety in the mesohydrobenzoin, having a strong $\pi-\pi$ interaction with one of the binaphthyl groups of the catalyst, might promote formation of the stereoselective product.

Based on the yield and enantioselectivity, the catalysts $\mathbf{Zn_2L_1}^{RR}$ and $\mathbf{Zn_2L_2}^{RR}$ were found to be efficient. Hence, we tested catalytic recyclability (Figure 7) using mesohydrobenzoin and benzoyl chloride as substrate. Interestingly, both $\mathbf{Zn_2L_1}^{RR}$ and $\mathbf{Zn_2L_2}^{RR}$, with amazing yield and *ee*, had catalytic efficiency that was retained up to seven cycles. The ^{1}H NMR

DOI: 10.1021/acs.inorgchem.8b03643
Inorg. Chem. XXXX, XXX, XXX−XXX

recorded for fresh and recycled catalyst of [$\mathbf{Zn_2L_1}^{RR}$] after the seventh cycle matching, confirming catalytic stability (Figure S38).

CONCLUSIONS

In summary, we have synthesized and characterized a series of terminally close-ended binuclear double-stranded helicates incorporating cupric acetates, zinc(II) acetate and zinc(II) chloride salts. The chirality transfer from ligand to metal monitored by the CD and ORDE was correlated for enantioselectivity on the asymmetric catalyst. The crystal structure obtained for racemic complex **3** followed a self-sorting behavior and revealed homochiral helicate pairs [**ΛΛ**-($\mathbf{Zn_2L_1}^{RR}(\mathbf{OAc})_2$)] and [**ΔΔ**-($\mathbf{Zn_2L_1}^{SS}(\mathbf{OAc})_2$)] in the unit cell. The enantiopure helicate **ΔΔ**-[$\mathbf{Zn_2L_1}^{SS}\mathbf{Cl_2}$] and the associated CD studies provide stereochemical compatibility and promote the desymmetrized product via enantioselective benzoylation. The self-sorting behavior of *rac*-BNDA leads to homochiral dimeric helicates [(ΔΔ)] and [(ΛΛ)]. Formation of (ΔΛ) heterochiral mesocate was found absent in the present analysis. The enantiopure catalysts **1′−4′** and **1″−4″** after synthesis were obtained as enantiopure compounds in ΛΛ and ΔΔ forms and are successfully applied for desymmetrization of C_2-symmetric mesodiols to achieve unsymmetrical monoesters with good yield (98%) and enantioselectivity (92%). Identifying the efficiency of these catalysts on asymmetric benzoylation of mesodiols, we have demonstrated the formation of symmetrical diols to monobenzoylated unsymmetrical diols through EDMD. The crystal structure and the systematic ^{1}H NMR studies in combination were used to derive a feasible mechanism for the desymmetrization of mesodiol. The recyclability and catalytic stability of the complexes investigated were satisfactory even after the seventh cycle.

EXPERIMENTAL SECTION

Materials and Methods. 4-Methyl-2,6-diformylphenol, 4-*tert*-butyl-2,6-diformylphenol, (*R*)-(+)-1,1′-binaphthyl-2,2′-diamine, (*S*)-(−)-1,1′-binaphthyl-2,2′-diamine, and cupric acetate monohydrate were purchased from Aldrich & Co. All these chemicals were used as received without any further purification. Microanalyses were done using a PerkinElmer PE 2400 series II CHNS/O elemental analyzer. IR spectra were recorded using KBr pellets (1% w/w) on a PerkinElmer Spectrum GX FT-IR spectrophotometer. Electronic spectra were recorded on a Shimadzu UV 3101 PC spectrophotometer. Mass analyses were performed using the positive electron spray ionization (ESI$^+$) technique on a waters Q TOF-micro mass spectrometer. ^{1}H and ^{13}C NMR spectra were recorded on a Bruker Avance DPX 200, 500 MHz and JEOL Delta 600 MHz FT-NMR spectrometer. Chemical shifts for proton resonances are reported in ppm (δ) relative to tetramethylsilane (TMS) and the ^{13}C is related to solvents. The CD spectra were recorded on a JASCO 815 Spectrometer. The enantioselectivity of the monobenzoylated product was determined by UFLC (Shimadzu SCL-10AVP) using chiral columns (Phenomenex Lux cellulose-1 and Amylose-2 column).

X-ray Crystallography. Summary of crystallographic data[34,35] and selected bond lengths and bond angles for **3.(OAc)$_2$** and [**3″.Cl$_2$**] are given in Table S3. Single-crystal X-ray data collection for **3** was performed on a Bruker SMART APEX CCD diffractometer equipped with graphite monochromatized Mo Kα radiation (λ = 0.71073 Å) at 150 K for [**3.(OAc)$_2$**]. No crystal decay was observed during the data collection. The SMART and SAINT software packages were used for data collection and reduction, respectively.[30] In all cases, absorption corrections based on multiscans using the SADABS software was also applied.[31] The structures were solved by direct methods SHELXTL and were refined on F^2 by the full-matrix least-squares technique.[32] All non-hydrogen atoms were refined anisotropically until convergence is reached. The hydrogen atoms were either located from difference Fourier map or fixed stereochemically. After the complete refinement of the of neutral dimeric Zn complex with one water and one acetonitrile molecule, diffuse peaks with residual electron density ranging from ∼3.5 Å^{-3} to 3 Å^{-3} were observed in the difference Fourier map, which can be attributed to a disordered solvent molecule present in the crystal lattice. Attempts to model these disordered peaks were unsuccessful since residual electron density was weak and there were no obvious major site occupations for the lattice solvent molecule. PLATON/SQUEEZE[33] was used to correct the diffraction data for the contribution from disordered lattice solvent (water) molecule. The solvent accessible void volume and the corresponding electron counts/unit cell estimated for [**3.(OAc)$_2$**] was 1004.4 Å^3 and 199 e Å^{-3}, respectively. This electron count corresponds to approximately nine disordered acetonitrile molecules present in the unit cell as a solvent of crystallization. Final cycles of least-squares refinements with the modified data set after subtracting the contribution from the disordered solvent molecules using SQUEEZ program significantly improved the *R*-values and Goodness of Fit of the structural data. The molecular formula provided in the crystallographic table is without incorporating the solvent molecules. Crystallographic data of [**3.(OAc)$_2$**] and [**3″.Cl$_2$**] has been deposited in the Cambridge Crystallographic Data Center as a supplementary publication with CCDC No. 1874548−1874549.

Synthesis of Helicate. *Copper Helicates.* 0.1 mmol of 4-methyl-2,6-diformylphenol for L_1 (16.4 mg) or 4-*tert*-butyl-2,6-diformylphenol for L_2 (20.6 mg) dissolved in acetonitrile (5 mL), 0.1 mmol of triethylamine (14 μL), and cupric acetate monohydrate (0.1 mmol, 19.9 mg) were mixed together and the solution was stirred constantly at room temperature for 30 min. Then, the *rac*-1,1′-binaphyl-2,2′-diamine (0.1 mmol, 28.4 mg) was added drop by drop. After the complete addition of the diamine, the solution slowly became a yellow to green color and the reaction mixture was refluxed for 36 h. Finally, the resulting dark brown solution was evaporated under rotavapor to remove the solvent and the residue was washed with dichloromethane (50 mL) and water (3 × 10 mL). The organic layer was separated and dried. Yield 84−85%.

*[$Cu_2L_1^{rac}(OAc)_2$] (**1**).* Yield 85%, UV−vis [(λ, nm) (ε/M^{-1})]: 245 (8414), 267 (7710), 286 (7270), 428 (4230), 662 (34) nm. FT-IR (KBr): ν = 3449, 3060, 3027, 2954, 2906, 2362, 1610, 1518, 1425, 1387, 1325, 1263, 1212, 1125, 1057, 756, 696 cm^{-1}. [ESI-MS]$^+$: Chemical formula for [M.OAc]$^+$ $C_{60}H_{41}Cu_2N_4O_4$, *m*/*z* Calc (found): 1007.17 (1007.85). Elemental Analysis: Mol. formula. $C_{62}H_{46}Cu_2N_4O_7$. Calc (found) C, 68.56 (68.13), H, 4.27 (4.78), N, 5.16 (5.62) %.

*[$Cu_2L_1^{RR}(OAc)_2$] (**1′**).* The above procedure was adopted and *R*-BNDA used instead of *rac*-BNDA. Yield 84%, UV−vis [(λ, nm) (ε/M^{-1})]: 247 (8310), 267 (7394), 288 (6970), 426 (4007), 664 (35) nm. FT-IR (KBr): ν = 3429, 3061, 3028, 2955, 2904, 2368, 1612, 1528, 1451, 1391, 1328, 1264, 1213, 1050, 833, 699 cm^{-1}. [ESI-MS]$^+$: Chemical Formula for [M.OAc]$^+$ $C_{60}H_{41}Cu_2N_4O_4$, *m*/*z* Calc (found): 1007.17 (1007.42). Elemental Analysis: Mol. formula. $C_{62}H_{48}Cu_2N_4O_8$. Calc (found) C, 67.44 (67.56), H, 4.38 (4.76), N, 5.07 (5.46) %.

*[$Cu_2L_1^{SS}(OAc)_2$] (**1″**).* Following the general procedure with *S*-BNDA used instead of *rac*-BNDA. Yield 85%, UV−vis [(λ, nm) (ε/M^{-1})]: 245 (8428), 267 (7459), 286 (6933), 428 (3879), 662 (33) nm. FT-IR (KBr): ν = 3449, 3060, 3027, 2954, 2906, 2362, 1610, 1518, 1425, 1387, 1325, 1263, 1212, 1125, 1057, 756, 696 cm^{-1}. [ESI-MS]$^+$: Chemical formula for [M.OAc]$^+$ $C_{60}H_{41}Cu_2N_4O_4$, *m*/*z* Calc (found): 1007.17 (1007.43). Elemental Analysis: Mol. formula. $C_{62}H_{46}Cu_2N_4O_7$. Calc (found) C, 68.56 (68.12), H, 4.27 (4.60), N, 5.16 (5.48) %.

*[$Cu_2L_2^{rac}(OAc)_2$] (**2**).* Following the general procedure using 4-methyl-2,6-diformylphenol and *rac*-BNDA. Yield 84%, UV−vis [(λ, nm) (ε/M^{-1})]: 245 (8485), 267 (7981), 286 (7654), 416 (4326), 669 (41) nm. FT-IR (KBr) ν = 3438, 3053, 2956, 2360, 1613, 1541, 1391, 1196, 1065, 818, 746, 688, 498 cm^{-1}. [ESI-MS]$^+$: Chemical

DOI: 10.1021/acs.inorgchem.8b03643
Inorg. Chem. XXXX, XXX, XXX−XXX

formula for $[M.OAc]^+$,$C_{66}H_{53}Cu_2N_4O_4$, *m/z* Calc (found) 1091.27 (1091.97). Elemental Analysis: Chemical Formula, $C_{68}H_{64}Cu_2N_4O_{10}$. Calc (found) C, 66.71 (66.92), H, 5.27 (5.65), N, 4.58 (4.12) %.

$[Cu_2L_2^{RR}(OAc)_2]$ (2′). Following the general procedure using 4-*tert*-butyl-2,6-diformylphenol and *R*-BNDA. Yield 85%, UV−vis [(λ, nm) (ε/M^{-1})]: 246 (8532), 266 (8133), 288 (7907), 414 (4190), 667 (38) nm. FT-IR (KBr): ν = 3432, 3053, 2962, 2362, 1607, 1541, 1385, 1199, 1059, 814, 750, 688, 492 cm^{-1}. $[ESI-MS]^+$: Chemical formula for $[M.OAc]^+$, $C_{66}H_{53}Cu_2N_4O_4$, *m/z* Calc (found) 1091.27 (1091.77). Elemental Analysis: Chemical Formula, $C_{68}H_{68}Cu_2N_4O_{12}$. Calc (found) C, 64.80 (64.35), H, 5.44 (5.103), N, 4.45 (4.43) %.

$[Cu_2L_2^{SS}(OAc)_2]$ (2″). Adapting the above general procedure and using 4-*tert*-butyl-2,6-diformylphenol and *S*-BNDA. Yield 84%, UV−vis [(λ, nm) (ε/M^{-1})]: 245 (8089), 267 (7740), 286 (7372), 416 (4289), 669 (33) nm. FT-IR (KBr): ν = 3438, 3053, 2956, 2360, 1613, 1541, 1391, 1196, 1065, 818, 746, 688, 498 cm^{-1}. $[ESI-MS]^+$: Chemical formula for $[M.OAc]^+$, $C_{66}H_{53}Cu_2N_4O_4$, *m/z* Calc (found) 1091.27 (1091.76). Elemental Analysis: Chemical Formula, $C_{68}H_{64}Cu_2N_4O_{10}$. Calc (found) C, 66.71 (66.28), H, 5.27 (5.383), N, 4.58 (4.72) %.

Zinc Helicates. The 4-methyl-2,6-diformylphenol for L_1 (16.4 mg, 0.1 mmol) or 4-*tert*-butyl-2,6-diformylphenol for L_2 (20.6 mg, 0.1 mmol) dissolved in acetonitrile (5 mL), triethylamine (14 μL, 0.1 mmol), and zinc acetate dehydrate (21.95 mg, 0.1 mmol) were mixed together, and the resultant solution was stirred constantly at room temperature for 0.5 h. Then 0.1 mmol of 1,1′-binaphyl-2,2′-diamine (28.4 mg) was added drop by drop. After the complete addition of diamine, the reaction mixture was refluxed for 36 h. Finally, from the yellow solution, the solvent was removed by rotavapor and the resulting residue was washed with dichloromethane (50 mL) and water (3 × 10 mL). The organic layer was separated and dried. Recrystallization from the acetonitrile yields yellow crystal which is suitable for single crystal XRD. Yield 84−85%.

$[Zn_2L_1^{rac}(OAc)_2]$ (3). Yield 84%. UV−vis [(λ, nm) (ε/M^{-1})]: 243 (8062), 269 (7616), 286 (7265), 412 (5204) nm. FT-IR (KBr): ν = 3429, 3060, 2923, 2369, 1629, 1548, 1391, 1326, 1209, 1065, 994, 818, 746, 668, 554, 485 cm^{-1}. ^1H NMR (500 MHz, CD_3OD, ppm): δ = 8.715 (s, 4H, −CH═N), 7.996−7.987 (m, 4H, −CH), 7.875−7.860 (m, 4H, −CH), 7.446−7.417 (m, 6H, −CH), 7.355−7.339 (m, 5H, −CH), 7.240−7.209 (m, 5H, −CH), 6.793−6.776 (m, 4H, −CH), 2.085 (s, 6H, $-CH_3$) 1.677 (s, 6H, $-CH_3$). ^{13}C NMR (125 MHz, CD_3OD, ppm): δ = 175.136, 169.965, 169.464, 165.583, 144.713, 144.059, 143.94, 142.668, 133.452, 131.723, 130.075, 128.622, 128.306, 128.220, 128.033, 127.124, 126.045, 125.77, 125.344, 124.564, 123.392, 123.176, 122.516, 121.065, 118.571, 22.394, 19.327. $[ESI-MS]^+$: Chemical formula for $[M.OAc]^+$, $C_{60}H_{41}N_4O_4Zn_2$, *m/z* Calc (found) 1011.17 (1011.34). Elemental Analysis: Chemical Formula, $C_{62}H_{48}N_4O_8Zn_2$. Calc (found) C, 67.22 (67.50), H, 4.37 (4.517), N, 5.06 (4.99) %.

$[Zn_2L_1^{RR}(OAc)_2]$ (3′). Similar procedure adopted above for $[(Zn_2L_1^{rac}(OAc)_2)]$ (3) and using *R*-BNDA instead of *rac*-BNDA. Yield 85%. UV−vis [(λ, nm) (ε/M^{-1})]: 245 (8549), 265 (6741), 290 (8343), 411 (6939) nm. FT-IR (KBr): ν = 3387, 3060, 2923, 2368, 1623, 1528, 1388, 1329, 1208, 1061, 1002, 872, 820, 748, 676, 538, 480 cm^{-1}. ^1H NMR (200 MHz, CD_3OD, ppm) δ = 8.651 (s, 4H, −CH═N), 7.916−7.783 (m, 8H, −CH), 7.459−7.387 (m, 4H, −CH), 7.333−7.146 (m, 12H, −CH), 6.823−6.780 (m, 4H, −CH), 1.998 (s, 6H, $-CH_3$) 1.661 (s, 6H, $-CH_3$). ^{13}C NMR (125 MHz, DMSO-d_6, ppm) δ = 174.936, 169.169, 165.636, 144.741, 142.637, 133.420, 131.707, 130.032, 128.605, 128.296, 128.207, 128.019, 127.094, 126.031, 125.772, 125.328, 124.486, 123.406, 123.166, 122.546, 121.048, 118.560, 110.491, 22.321, 19.326. $[ESI-MS]^+$: Chemical formula for $[M.OAc]^+$, $C_{60}H_{41}N_4O_4Zn_2$, *m/z* Calc (found) 1011.17 (1011.69). Elemental Analysis: Chemical Formula, $C_{62}H_{52}N_4O_{10}Zn_2$. Calc (found) C, 65.10 (65.81), H, 4.58 (4.41), N, 4.90 (4.88) %.

$[Zn_2L_1^{SS}(OAc)_2]$ (3″). Similar procedure adopted above for $[(Zn_2L_1^{rac}(OAc)_2)]$ (3) and using *S*-BNDA instead of *rac*-BNDA. Yield 83%. UV−vis [(λ, nm) (ε/M^{-1})]: 243 (7372), 269 (6814), 286 (6392), 412 (4119) nm. FT-IR (KBr): ν = 3429, 3060, 2923, 2369, 1629, 1548, 1391, 1326, 1209, 1065, 994, 818, 746, 668, 554, 485 cm^{-1}. ^1H NMR (200 MHz, CD_3OD, ppm): δ = 8.702(s, 4H, −CH═N), 7.989−7.834 (m, 8H, −CH), 7.435−7.233(m, 16H, −CH), 6.810−6.768 (m, 4H, −CH), 2.066 (s, 6H, $-CH_3$) 1.688 (s, 6H, $-CH_3$). ^{13}C NMR (125 MHz, DMSO-d_6, ppm) δ = 174.968, 169.931, 165.628, 144.732, 144.055, 143.890, 142.638, 133.426, 131.708, 130.033, 128.296, 128.207, 127.102, 125.768, 125.339, 124.507, 123.402, 123.168, 122.539, 121.056, 118.563, 22.325, 19.322. $[ESI-MS]^+$: Chemical formula for $[M.OAc]^+$, $C_{60}H_{41}N_4O_4Zn_2$, *m/z* Calc (found) 1011.17 (1011.57). Elemental Analysis: Chemical Formula, $C_{62}H_{48}N_4O_8Zn_2$. Calc (found) C, 67.22 (67.50), H, 4.37 (4.52), N, 5.06 (4.99) %.

$[Zn_2L_2^{rac}(OAc)_2]$ (4). 4-*tert*-Butyl-2,6-diformylphenol used instead of 4-methyl-2,6-diformylphenol and *rac*-BNDA. Yield 84%. UV−vis [(λ, nm) (ε/M^{-1})]: 246 (8465), 268 (6843), 289 (6420), 406 (4011) nm. FT-IR (KBr): ν = 3429, 3060, 2923, 2369, 1629, 1548, 1391, 1326, 1209, 1065, 994, 818, 746, 668, 554, 485 cm^{-1}. ^1H NMR (500 MHz, CD_3OD, ppm): δ = 8.893 (s, 4H, −CH═N), 8.145−8.128 (m, 4H, −CH), 7.975−7.958 (m, 4H, −CH), 7.801−7.769 (m, 4H, −CH), 7.444−7.398 (m, 6H, −CH), 7.234−7.205 (m, 6H, −CH), 6.777−6.760 (m, 4H, −CH), 1.708 (s, 6H, $-CH_3$) 1.250 (s, 18H, $-C(CH_3)_3$). ^{13}C NMR (125 MHz, CD_3OD, ppm): δ = 174.992, 170.591, 165.453, 144.802, 144.055, 139.831, 138.321, 133.483, 131.767, 130.073, 128.613, 128.293, 128.023, 127.084, 126.031, 125.786, 125.330, 123.519, 123.174, 122.222, 121.055, 118.563, 110.505, 33.657, 30.970, 30.866, 22.414. $[ESI-MS]^+$: Chemical formula for $[M.OAc]^+$, $C_{60}H_{41}N_4O_4Zn_2$. *m/z* Calc (found) 1093.27 (1093.49). Elemental Analysis: Chemical Formula, $C_{68}H_{66}N_4O_{11}Zn_2$. Calc (found) C, 65.55 (65.07), H, 5.34 (4.65), N, 4.50 (4.55) %.

$[Zn_2L_2^{RR}(OAc)_2]$ (4′). Similar procedure adopted above except *R*-BNDA instead of *rac*-BNDA. Yield 85%. UV−vis [(λ, nm) (ε/M^{-1})]: 244 (7607), 269 (7168), 289 (6839), 409 (4251) nm. FT-IR (KBr): ν = 3387, 3060, 2923, 2368, 1623, 1528, 1388, 1329, 1208, 1061, 1002, 872, 820, 748, 676, 538, 480 cm^{-1}. ^1H NMR (200 MHz, CD_3OD, ppm): δ = 8.877 (s, 4H, −CH═N), 8.144−8.101 (m, 4H, −CH), 7.977−7.937 (m, 4H, −CH), 7.779 (m, 4H, −CH), 7.481−7.373 (m, 6H, −CH), 7.247−7.172 (m, 6H, −CH), 6.797−6.754 (m, 4H, −CH), 1.705 (s, 6H, $-CH_3$), 1.242 (s, 18H, $-C(CH_3)_3$). ^{13}C NMR (125 MHz, DMSO-d_6, ppm) δ = 174.978, 170.607, 165.475, 144.818, 144.065, 139.840, 138.336, 133.493, 131.779, 130.088, 128.631, 128.305, 128.262, 128.039, 127.098, 126.049, 125.798, 123.528, 123.185, 122.237, 121.073, 118.576, 110.519, 33.670, 30.982, 30.879, 22.422. $[ESI-MS]^+$: Chemical formula for $[M.OAc]^+$, $C_{60}H_{41}N_4O_4Zn_2$, *m/z* Calc (found) 1093.27 (1093.46). Elemental Analysis: Chemical Formula, $C_{68}H_{60}N_4O_8Zn_2$. Calc (found) C, 68.52 (68.37), H, 5.07 (5.02), N, 4.70 (4.75) %.

$[Zn_2L_2^{SS}(OAc)_2]$ (4″). Similar procedure adopted above except *S*-BNDA instead of *rac*-BNDA. Yield 84%. UV−vis [(λ, nm) (ε/M^{-1})]: 246 (8451), 268 (7713), 289 (7298), 406 (3791) nm. FT-IR (KBr): ν = 3429, 3060, 2923, 2369, 1629, 1548, 1391, 1326, 1209, 1065, 994, 818, 746, 668, 554, 485 cm^{-1}. ^1H NMR (200 MHz, CD_3OD, ppm): δ = 8.883 (s, 4H, −CH═N), 8.139−8.096 (m, 4H, −CH), 7.976−7.936 (m, 4H, −CH), 7.810−7.786 (m, 6H, −CH), 7.477−7.365 (m, 6H, −CH), 7.245−7.134 (m, 4H, −CH), 6.796−6.750 (m, 4H, −CH), 1.690 (s, 6H, $-CH_3$) 1.238 (s, 18H, $-C(CH_3)_3$). ^{13}C NMR (125 MHz, DMSO-d_6, ppm) δ = 174.884, 170.581, 165.455, 144.802, 144.051, 139.824, 138.291, 133.468, 131.756, 130.056, 128.600, 128.290, 128.013, 127.076, 126.023, 125.776, 125.316, 123.513, 123.165, 122.221, 121.040, 118.554, 110.487, 33.653, 30.968, 30.862, 22.387. $[ESI-MS]^+$: Chemical formula for $[M.OAc]^+$, $C_{60}H_{41}N_4O_4Zn_2$, *m/z* Calc (found) 1093.27 (1093.47). Elemental Analysis: Chemical Formula, $C_{68}H_{64}N_4O_{10}Zn_2$. Calc (found) C, 66.51 (66.37), H, 5.25 (5.67), N, 4.56 (4.83) %.

$[Zn_2L_2^{SS}Cl_2]$ (4″.Cl_2). Similar procedure adopted above except *S*-BNDA and zinc chloride instead of *rac*-BNDA and zinc acetate. Yield 83%. UV−vis [(λ, nm) (ε/M^{-1})]: 247 (8321), 266 (7642), 288 (7341), 404 (3625) nm. FT-IR (KBr): ν = 3430, 3056, 2918, 2365, 1625, 1545, 1386, 1322, 1204, 1061, 992, 815, 744, 665, 552, 482 cm^{-1}. ^1H NMR (600 MHz, DMSO-d_6, ppm): δ = 8.855(s, 4H, −CH═N), 8.176−8.162 (d, *J* = 9 Hz, 4H, −CH), 8.043−8.029 (d, *J*

DOI: 10.1021/acs.inorgchem.8b03643
Inorg. Chem. XXXX, XXX, XXX−XXX

= 8 Hz, 4H, −CH), 7.652 (s, 4H, −CH), 7.487−7.462 (t, J = 8 Hz, 4H, −CH), 7.395−7.381 (d, J = 8 Hz, 4H, −CH), 7.274−7.249 (t, J = 8 Hz, 4H, −CH), 6.676−6.662 (d, J = 9 Hz, 4H, −CH) 2.160 (s, 6H, $-CH_3$). ^{13}C NMR (125 MHz, DMSO-d_6, ppm) δ = 170.604, 144.556, 144.101, 139.523, 138.656, 133.231, 131.665, 130.012, 128.544, 128.222, 128.102, 127.978, 127.565, 126.415, 125.333, 125.103, 123.458, 123.159, 122.656, 121.858, 118.333, 110.942, 22.356. [ESI-MS]$^+$: Chemical formula for [M.Cl]$^+$, $C_{58}H_{38}ClN_4O_2Zn_2$, m/z Calc (found) 987.12 (987.43). Elemental Analysis: Chemical Formula, $C_{58}H_{42}Cl_2N_4O_4Zn_2$. Calc (found) C, 65.68 (65.89), H, 3.99 (3.54), N, 5.28 (5.62) %.

General Procedure for Desymmetrization of Mesodiols. A dry and nitrogen flushed 5 mL flask, equipped with a magnetic stirring bar, was charged with zinc(II) catalyst (2 mol %) and freshly distilled dry DCM (2 mL). Corresponding diol (0.2 mmol), and 2 equiv *N*,*N*-diisopropylethylamine (DIPEA) (0.4 mmol) were then added successively, and the resulting mixture was stirred up to 10−15 min and benzoyl chloride (0.2 mmol) was added slowly by syringe at 0 °C. The mixture was stirred at the same temperature until completion of the reaction. The reaction was monitored by TLC. After completion of the reaction, the solvent was evaporated by rotavapor and washed with hexane/EtOAc (90/10%) to separate catalyst from the mixture (8 times). Finally, the crude product was purified by column chromatography (silica gel: 100−200 mesh using ethyl acetate and hexanes) to give corresponding monoester product. Enantiomeric excess was determined by UFLC using Phenomenox Lux cellulose-1 and Amylose-2 column using isopropanol and hexane as eluting agent. The absolute configurations of the products were assigned by comparison HPLC profile with the reported literature.[36]

■ ASSOCIATED CONTENT

Supporting Information

The Supporting Information is available free of charge on the ACS Publications website at DOI: 10.1021/acs.inorgchem.8b03643.

Characterization of all the complexes such as ESI-MS, NMR, UV−vis, FT-IR, crystal data; and characterization of catalytic products (PDF)

Accession Codes

CCDC 1874548−1874549 contain the supplementary crystallographic data for this paper. These data can be obtained free of charge via www.ccdc.cam.ac.uk/data_request/cif, or by emailing data_request@ccdc.cam.ac.uk, or by contacting The Cambridge Crystallographic Data Centre, 12 Union Road, Cambridge CB2 1EZ, UK; fax: +44 1223 336033.

■ AUTHOR INFORMATION

Corresponding Author

*E-mail: siva@csmcri.res.in or siva140@yahoo.co.in.

ORCID

Eswaran Chinnaraja: 0000-0003-0617-2316
Eringathodi Suresh: 0000-0002-1934-6832
Ramalingam Natarajan: 0000-0002-8281-7158
Palani S. Subramanian: 0000-0002-9035-0973

Notes

The authors declare no competing financial interest.

■ ACKNOWLEDGMENTS

CSMCRI communication number CSIR-CSMCRI 181/2018. Author EC and RA acknowledge the CSIR for SRF grants. The authors gratefully acknowledge DST-SERB New Delhi (Project No. SR/S1/IC-23/2011) for funding. Members of ADCIF of CSMCRI are acknowledged for their instrumentation support.

■ REFERENCES

(1) (a) Ciuffreda, P.; Alessandrini, L.; Terraneo, G.; Santaniello, E. Lipase-Catalyzed Selective Benzoylation of 1,2-diols with Vinyl Benzoate in Organic Solvents. *Tetrahedron: Asymmetry* **2003**, *14*, 3197−3201. (b) Juárez-Hernandez, M.; Johnson, D. V.; Holland, H. L.; McNulty, J.; Capretta, A. Lipase-Catalyzed Stereoselective Resolution and Desymmetrization of Binaphthols. *Tetrahedron: Asymmetry* **2003**, *14*, 289−291. (c) Nakatake, D.; Yokote, Y.; Matsushima, Y.; Yazaki, R.; Ohshima, T. A Highly Stable but Highly Reactive Zinc Catalyst for Transesterification Supported by a Bis(imidazole) Ligand. *Green Chem.* **2016**, *18*, 1524−1530.

(2) (a) Fujimoto, Y.; Iwadate, H.; lkekawa, N. Preparation of Optically Active 2,2′-Dihydroxy-1,1′-binaphthyl *via* Microbial Resolution of the Corresponding Racemic Diester. *J. Chem. Soc., Chem. Commun.* **1985**, 1333−1334. (b) Köhler, J.; Wünsch, B. Lipase Catalyzed Enantioselective Desymmetrization of a Prochiral Pentane-1,3,5-triol Derivative. *Tetrahedron: Asymmetry* **2006**, *17*, 3091−3099. (c) Schätz, A.; Grass, R. N.; Kainz, Q.; Stark, W. J.; Reiser, O. Cu(II)-Azabis(oxazoline) Complexes Immobilized on Magnetic Co/C Nanoparticles: Kinetic Resolution of 1,2-Diphenylethane-1,2-diol under Batch and Continuous-Flow Conditions. *Chem. Mater.* **2010**, *22*, 305−310.

(3) (a) Enríquez-Garcíaw, Á.; Kündig, E. P. Desymmetrisation of *meso*-diols Mediated by Non-enzymatic Acyl Transfer Catalysts. *Chem. Soc. Rev.* **2012**, *41*, 7803−7831. (b) Vedejs, E.; Daugulis, O.; Tuttle, N. Desymmetrization of *meso*-Hydrobenzoin Using Chiral, Nucleophilic Phosphine Catalysts. *J. Org. Chem.* **2004**, *69*, 1389−1392.

(4) (a) Iwasaki, F.; Maki, T.; Onomura, O.; Nakashima, W.; Matsumura, Y. Chemo- and Stereoselective Monobenzoylation of 1,2-Diols Catalyzed by Organotin Compounds. *J. Org. Chem.* **2000**, *65*, 996−1002. (b) Maigrot, N.; Mazaleyrat, J. P. New and Improved Synthesis of Optically Pure (*R*)-and (*S*)-2,2′-Dimethyl-1, 1′-binaphthyl and Related Compounds. *Synthesis* **1985**, *1985*, 317−320. (c) Iwasaki, F.; Maki, T.; Nakashima, W.; Onomura, O.; Matsumura, Y. Nonenzymatic Kinetic Resolution of 1,2-Diols Catalyzed by an Organotin Compound. *Org. Lett.* **1999**, *1*, 969−972.

(5) (a) Ishihara, K.; Kubota, M.; Yamamoto, H. First Application of Hydrogen Bonding Interactions to the Design of Asymmetric Acylation of *Meso*-Diols with Optically Active Acyl Halides. *Synlett* **1994**, *1994*, 611−614. (b) Oriyama, T.; Imai, K.; Hosoya, T.; Sano, T. Asymmetric Acylation of *meso*-diols with Benzoyl Halide in the Presence of a Chiral Diamine. *Tetrahedron Lett.* **1998**, *39*, 397−400.

(6) (a) Wurz, R. P. Chiral Dialkylaminopyridine Catalysts in Asymmetric Synthesis. *Chem. Rev.* **2007**, *107*, 5570−5595. (b) Fu, G. C. Enantioselective Nucleophilic Catalysis with "Planar-Chiral" Heterocycles. *Acc. Chem. Res.* **2000**, *33*, 412−420. (c) Fu, G. C. Asymmetric Catalysis with "Planar-Chiral" Derivatives of 4-(Dimethylamino)pyridine. *Acc. Chem. Res.* **2004**, *37*, 542−547. (d) Ie, Y.; Fu, G. C. A New Benchmark for the Non-Enzymatic Enantioselective Acylation of Amines: Use of a Planar-Chiral Derivative of 4-Pyrrolidinopyridine as the Acylating Agent. *Chem. Commun.* **2000**, 119−120. (e) Spivey, A. C.; Fekner, T.; Spey, S. E. Axially Chiral Analogues of 4-(Dimethylamino)pyridine: Novel Catalysts for Nonenzymatic Enantioselective Acylations. *J. Org. Chem.* **2000**, *65*, 3154−3159.

(7) (a) Terakado, D.; Oriyama, T. Catalytic Asymmetric Acylation of Alcohols Using a Chiral 1,2-Diamine Derived from (S)-Proline: (1S,2S)-Trans-1-Benzoyloxy-2-Bromocyclohexane. *Org. Synth.* **2006**, *83*, 70−79. (b) Oriyama, T.; Taguchi, H.; Terakado, D.; Sano, T. Highly Efficient and Enantioselective Method for the Synthesis of Chiral Building Blocks Derived from *meso*-1,3-Propanediols. *Chem. Lett.* **2002**, *31*, 26−27.

(8) (a) Vedejs, E.; Daugulis, O.; Tuttle, N. Desymmetrization of *meso*-Hydrobenzoin Using Chiral, Nucleophilic Phosphine Catalysts. *J. Org. Chem.* **2004**, *69*, 1389−1392. (b) Holz, J.; Zayas, O.; Jiao, H.; Baumann, W.; Spannenberg, A.; Monsees, A.; Riermeier, T. H.; Almena, J.; Kadyrov, R.; Börner, A. A Highly Tunable Family of

DOI: 10.1021/acs.inorgchem.8b03643
Inorg. Chem. XXXX, XXX, XXX−XXX

Chiral Bisphospholanes for Rh-Catalyzed Enantioselective Hydrogenation Reactions. *Chem. - Eur. J.* **2006**, *12*, 5001−5013.
(9) (a) Mizuta, S.; Sadamori, M.; Fujimoto, T.; Yamamoto, I. Asymmetric Desymmetrization of *meso*-1,2-Diols by Phosphinite Derivatives of Cinchona Alkaloids. *Angew. Chem., Int. Ed.* **2003**, *42*, 3383−3385. (b) Mizuta, S.; Tsuzuki, T.; Fujimoto, T.; Yamamoto, I. Catalytic Asymmetric Desymmetrization of Cyclic *meso*-1,3- and 1,4-Diols by a Phosphinite Derivative of Quinidine. *Org. Lett.* **2005**, *7*, 3633−3635.
(10) Lewis, C. A.; Sculimbrene, B. R.; Xu, Y.; Miller, S. J. Desymmetrization of Glycerol Derivatives with Peptide-Based Acylation Catalysts. *Org. Lett.* **2005**, *7*, 3021−3023.
(11) Nagumo, S.; Arai, T.; Akita, H. Synthetic Study of Tautomycin. I Synthesis and Regioseleetive Enzymatic Acetylation of a Spiroketal Diol Related to the C_5-C_{16} Fragment. *Tetrahedron Lett.* **1997**, *38*, 5165−5168.
(12) Kim, H. C.; Youn, J.-H.; Kang, S. H. Synthesis of *L*-Cladinose Using Enantioselective Desymmetrization. *Synlett* **2008**, *2008*, 2526−2528.
(13) (a) Iwasaki, F.; Maki, T.; Onomura, O.; Nakashima, W.; Matsumura, Y. Chemo- and Stereoselective Monobenzoylation of 1,2-Diols Catalyzed by Organotin Compounds. *J. Org. Chem.* **2000**, *65*, 996−1002. (b) Arai, T.; Mizukami, T.; Yanagisawa, A. Reaction Optimization Using Solid-Phase Catalysis-CD HTS: *N*b-Imidazoline−Cu(I)-Catalyzed Asymmetric Benzoylation of 1,2-Diols. *Org. Lett.* **2007**, *9*, 1145−1147.
(14) (a) Trost, B. M.; Mino, T. Desymmetrization of Meso 1,3- and 1,4-Diols with a Dinuclear Zinc Asymmetric Catalyst. *J. Am. Chem. Soc.* **2003**, *125*, 2410−2411. (b) Trost, B. M.; Chan, V. S.; Yamamoto, D. Enantioselective ProPhenol-Catalyzed Addition of 1,3-Diynes to Aldehydes to Generate Synthetically Versatile Building Blocks and Diyne Natural Products. *J. Am. Chem. Soc.* **2010**, *132*, 5186−5192.
(15) Suzuki, T. Recent Topics in the Desymmetrization of *meso*-diols. *Tetrahedron Lett.* **2017**, *58*, 4731−4739.
(16) (a) Albrecht, M.; Blau, O.; Fröhlich, R. Size-selectivity" in the template-directed assembly of dinuclear triple-stranded helicates. *Proc. Natl. Acad. Sci. U. S. A.* **2002**, *99*, 4867−4872. (b) Hamblin, J.; Childs, L. J.; Alcock, N. W.; Hannon, M. J. Directed one-pot syntheses of enantiopure dinuclear silver(I) and copper(I) metallo-supramolecular double helicates. *J. Chem. Soc., Dalton Trans.* **2002**, 164−169. (c) Albrecht, M. Let's Twist Again"−Double-Stranded, Triple-Stranded, and Circular Helicates. *Chem. Rev.* **2001**, *101* (11), 3457−3498.
(17) (a) Yeh, R. M.; Raymond, K. N. Supramolecular Asymmetric Induction in Dinuclear Triple-Stranded Helicates. *Inorg. Chem.* **2006**, *45*, 1130−1139. (b) Howson, S. E.; Bolhuis, A.; Brabec, V.; Clarkson, G. J.; Malina, J.; Rodger, A.; Scott, P. Optically pure, water-stable metallo-helical 'flexicate' assemblies with antibiotic activity. *Nat. Chem.* **2012**, *4*, 31−36. (c) Crassous, J. Chiral transfer in coordination complexes: towards molecular materials. *Chem. Soc. Rev.* **2009**, *38*, 830−845. (d) Crassous, J. Transfer of chirality from ligands to metal centers: recent examples. *Chem. Commun.* **2012**, *48*, 9684−9692.
(18) (a) Owens, T. D.; Souers, A. J.; Ellman, J. A. The Preparation and Utility of Bis(sulfinyl)imidoamidine Ligands for the Copper-Catalyzed Diels-Alder Reaction. *J. Org. Chem.* **2003**, *68*, 3−10. (b) Kwong, H.-L.; Yeung, H.-L.; Lee, W.-S.; Wong, W.-T. Stereoselective formation of a single-stranded helicate: Structure of a bis(palladium-allyl)quaterpyridine complex and its use in catalytic enantioselective allylic substitution. *Chem. Commun.* **2006**, 4841−4843. (c) Sham, K.-C.; Yeung, H.-L.; Yiu, S.-M.; Lau, T.-C.; Kwong, H.-L. New binuclear double-stranded manganese helicates as catalysts for alkene epoxidation†. *Dalton Trans* **2010**, *39*, 9469−9471. (d) Yeung, C.-T.; Yeung, H.-L.; Tsang, C.-S.; Wong, W.-Y.; Kwong, H.-L. Supramolecular double helical Cu(I) complexes for asymmetric cyclopropanation. *Chem. Commun.* **2007**, 5203−5205.
(19) Telfer, S. G.; Sato, T.; Harada, T.; Kuroda, R.; Lefebvre, J.; Leznoff, D. B. Mono- and Dinuclear Complexes of Chiral Tri- and Tetradentate Schiff-Base Ligands Derived from 1,1'-Binaphthyl-1,1'-diamine. *Inorg. Chem.* **2004**, *43*, 6168−6176.
(20) (a) Arunachalam, R.; Chinnaraja, E.; Valkonen, A.; Rissanen, K.; Sen, S. K.; Natarajan, R.; Subramanian, P. S. Enantiomeric resolution of asymmetric-carbon-free binuclear double-stranded cobalt(III) helicates and their application as catalysts in asymmetric reactions. *Inorg. Chem.* **2018**, *57* (18), 11414−11421. (b) Faulkner, A. D.; Kaner, R. A.; Abdallah, Q. M. A.; Clarkson, G.; Fox, D. J.; Gurnani, P.; Howson, S. E.; Phillips, R. M.; Roper, D. I.; Simpson, D. H.; Scott, P. Asymmetric Triplex Metallohelices with High and Selective Activity Against Cancer Cells. *Nat. Chem.* **2014**, *6*, 792−803. (c) Albrecht, M. Making head−head-tails of it. *Nat. Chem.* **2014**, *6*, 761−762.
(21) (a) Albrecht, M.; Kotila, S. Formation of a "*meso*−Helicate" by Self−Assembly of Three Bis(catecholate) Ligands and Two Titanium-(IV) Ions. *Angew. Chem., Int. Ed. Engl.* **1995**, *34* (19), 2134−2137. (b) Xu, J.; Parac, T. N.; Raymond, K. N. *meso* Myths: What Drives Assembly of Helical versus *meso*-$[M_2L_3]$ Clusters? *Angew. Chem., Int. Ed.* **1999**, *38* (19), 2878−2882. (c) Cui, F.; Li, S.; Jia, C.; Mathieson, J. S.; Cronin, L.; Yang, X.-J.; Wu, B. Anion-Dependent Formation of Helicates versus Mesocates of Triple-Stranded M_2L_3 (M = Fe^{2+}, Cu^{2+}) Complexes. *Inorg. Chem.* **2012**, *51*, 179−187.
(22) Telfer, S. G.; Sato, T.; Harada, T.; Kuroda, R.; Lefebvre, J.; Leznoff, D. B. Mono- and Dinuclear Complexes of Chiral Tri- and Tetradentate Schiff-Base Ligands Derived from 1,1'-Binaphthyl-2,2'-diamine. *Inorg. Chem.* **2004**, *43*, 6168−6176.
(23) (a) Telfer, S. G.; Sato, T.; Kuroda, R. Noncovalent Ligand Strands for Transition-Metal Helicates: The Straightforward and Stereoselective Self-Assembly of Dinuclear Double-Stranded Helicates Using Hydrogen Bonding. *Angew. Chem., Int. Ed.* **2004**, *43*, 581−584. (b) Constable, E. C.; Kulke, T.; Neuburger, M.; Zehnder, M. Diastereoselective formation of P and M dicopper(I) double helicates with chiral 2,2′:6′,2″-terpyridines. *Chem. Commun.* **1997**, 489−490.
(24) (a) Provent, C.; Bernardinelli, G.; Williams, A. F.; Vulliermet, N. Diastereoselectivity of Octahedral Cobalt(II) Pybox Complexes. *Eur. J. Inorg. Chem.* **2001**, *2001*, 1963−1967. (b) Pfukwa, R.; Kouwer, P. H. J.; Rowan, A. E.; Klumperman, B. Templated Hierarchical Self-Assembly of Poly (*p* -aryltriazoles) Foldamers. *Angew. Chem.* **2013**, *125*, 11246−11250.
(25) (a) Brunel, J. M. Update 1 of: BINOL: A Versatile Chiral Reagent. Chem. Rev. 2007, 107 (9), PR1−PR45. BINOL: A Versatile Chiral Reagent. Chem. Rev. 2005, 105 (3), 857−898. Update 1 of: BINOL: A Versatile Chiral Reagent. (Chem. Rev. 2007, 107, PR1−PR45. Published on the Web September 12, 2007.). *Chem. Rev.* **2008**, *108*, 1170−1170. (b) Kumarasamy, E.; Raghunathan, R.; Sibi, M. P.; Sivaguru, J. Nonbiaryl and Heterobiaryl Atropisomers: Molecular Templates with Promise for Atropselective Chemical Transformations. *Chem. Rev.* **2015**, *115*, 11239−11300. (c) Wang, Y.-B.; Tan, B. Construction of Axially Chiral Compounds via Asymmetric Organocatalysis. *Acc. Chem. Res.* **2018**, *51*, 534−547.
(26) (a) Crassous, J. Chiral Transfer in Coordination Complexes: Towards Molecular Materials. *Chem. Soc. Rev.* **2009**, *38*, 830−845. (b) Ousaka, N.; Takeyama, Y.; Iida, H.; Yashima, E. Chiral Information Harvesting in Dendritic Metallopeptides. *Nat. Chem.* **2011**, *3*, 856−861. (c) He, C.; Zhao, Y.; Guo, D.; Lin, Z.; Duan, C. Chirality Transfer through Helical Motifs in Coordination Compounds. *Eur. J. Inorg. Chem.* **2007**, *2007*, 3451−3463. (d) Crassous, J. Transfer of chirality from ligands to metal centers: recent examples. *Chem. Commun.* **2012**, *48*, 9687−9695.
(27) (a) Knof, U.; von Zelewsky, A. Predetermined Chirality at Metal Centers. *Angew. Chem., Int. Ed.* **1999**, *38*, 302−322. (b) Fujiki, M. Supramolecular Chirality: Solvent Chirality Transfer in Molecular Chemistry and Polymer Chemistry. *Symmetry* **2014**, *6*, 677−703. (c) He, C.; Zhao, Y.; Guo, D.; Lin, Z.; Duan, C. Chirality Transfer through Helical Motifs in Coordination Compounds. *Eur. J. Inorg. Chem.* **2007**, *2007*, 3451−3463.
(28) (a) Matsumura, Y.; Maki, T.; Murakami, S.; Onomura, O. Copper Ion-Induced Activation and Asymmetric Benzoylation of 1,2-Diols: Kinetic Chiral Molecular Recognition. *J. Am. Chem. Soc.* **2003**, *125*, 2052−2053. (b) Spivey, A. C.; Zhu, F.; Mitchell, M. B.; Davey, S. G.; Jarvest, R. L. Concise Synthesis, Preparative Resolution, Absolute

DOI: 10.1021/acs.inorgchem.8b03643
Inorg. Chem. XXXX, XXX, XXX−XXX

Configuration Determination, and Applications of an Atropisomeric Biaryl Catalyst for Asymmetric Acylation. *J. Org. Chem.* **2003**, *68*, 7379−7385. (c) Kawabata, T.; Nagato, M.; Takasu, K.; Fuji, K. Nonenzymatic Kinetic Resolution of Racemic Alcohols through an "Induced Fit" Process. *J. Am. Chem. Soc.* **1997**, *119*, 3169−3170.

(29) Pennington, W. T.; Chakraborty, S.; Paul, I. C.; Curtin, D. Y. Crystal Structures of D-(+)- and meso-Hydrobenzoin. Absolute Direction of the Dipole Moment of D- and L-Hydrobenzoin in the Crystal and Correlation with Crystal Morphology, Pyroelectric Effect, and Absolute Configuration. *J. Am. Chem. Soc.* **1988**, *110*, 6498−6504.

(30) Sheldrick, G. M. *SAINT S*, 1st ed.; Siemens Industrial Automation Inc., Madison, WI, 1995.

(31) *SADABS, Empirical Absorption Correction Program*; University of Göttingen, Göttingen, Germany, 1997.

(32) Sheldrick, G. M. *SHELXTL Reference Manual: Version 5.1*; Bruker AXS, Madison, WI, 1997.

(33) Spek, A. L. Structure validation in chemical crystallography. *Acta Crystallogr., Sect. D: Biol. Crystallogr.* **2009**, *65*, 148−155.

(34) Complex **3**: CCDC 1874548. Crystal data for $C_{64}H_{49}Cl_2N_5O_7Zn_2$ (M = 1130.82 g/mol): monoclinic, space group $P2_1/n$, a = 12.4323(12) Å, b = 24.785(3) Å, c = 19.267(2) Å, V = 5873.0(10) Å^3, Z = 4, T = 150.0(2) K, μ(Mo Kα) (λ = 0.71073 Å) mm^{-1}, D_{calc} = 1.279 g/cm^3, 13258 reflections measured ($1.35° \leq 2\Theta \leq 27.59°$), 34643 unique ($R_{int}$ = 0.0446; R_σ = 0.0651) which were used in all calculations. The final R_1 was 0.0764 [$I > 2\sigma(I)$] and wR_2 was 0.1179 (all data).

(35) Complex **3″**: CCDC 1874549. Crystal data for $C_{68}H_{53}Cl_2N_9O_2Zn_2$ (M = 1229.83 g/mol): monoclinic, space group C_2, a = 21.467(2) Å, b = 27.811(3) Å, c = 10.7501(10) Å, V = 6418.2(10) Å^3, Z = 4, T = 100.0 K, μ(Mo Kα) (λ = 0.71073 Å) mm^{-1}, D_{calc} = 1.273 g/cm^3, 46266 reflections measured ($3.794° \leq 2\Theta \leq 55.758°$), 14702 unique ($R_{int}$ = 0.1119; R_σ = 0.1561) which were used in all calculations. The final R_1 was 0.0935 [$I \geq 2\sigma(I)$] and wR_2 was 0.2756 (all data), Flack parameter = 0.03(2).

(36) (a) Nakamura, D.; Kakiuchi, K.; Koga, K.; Shirai, R. Design and Synthesis of Novel C_2-Symmetric Chiral Piperazines and an Application to Asymmetric Acylation of σ-Symmetric 1,2-Diols. *Org. Lett.* **2006**, *8*, 6139−6142. (b) Aida, H.; Mori, K.; Yamaguchi, Y.; Mizuta, S.; Moriyama, T.; Yamamoto, I.; Fujimoto, T. Enantioselective Acylation of 1,2- and 1,3-Diols Catalyzed by Aminophosphinite Derivatives of (1*S*,2*R*)-1-Amino-2-indanol. *Org. Lett.* **2012**, *14*, 812−815.

DOI: 10.1021/acs.inorgchem.8b03643
Inorg. Chem. XXXX, XXX, XXX−XXX